TOWARDS A LINEAR ENGINE

A THESIS
SUBMITTED TO THE DEPARTMENT OF MECHANICAL ENGINEERING
AND THE COMMITTEE ON GRADUATE STUDIES
OF STANFORD UNIVERSITY
IN PARTIAL FULFILLMENT OF THE REQUIREMENTS
FOR THE DEGREE OF
ENGINEER

Michael Anthony Prados

May 2002

Approved for the Department:

J. Christian Gerdes
(Principal Adviser)

Approved for the University Committee on Graduate Studies:

Abstract

Research towards improving the performance of internal combustion engines is important because they are ubiquitous. For the common scenario of engines which are used solely to generate electrical power, it is possible to replace the crankshaft, which translates linear motion into rotary motion, with a linear electrical machine, which transforms linear motion into electrical power. This technology is advantageous because it is mechanically simpler and allows for a great deal more freedom in defining a piston motion profile, enabling the use of novel combustion regimes.

After reviewing previous research at West Virginia University, Sandia National Labs, and the University of Regina, the representatives of the labs involved decided that this linear engine should use a four stroke working cycle, that it should consist of a single unopposed cylinder, and that it should be of comparable scale to existing research engines. A simulation was developed in Matlab Simulink, modelling the thermodynamic system, the electrical system, and the mechanical system. Based on initial results of this simulation, a linear electric motor was chosen as the cornerstone of the engine. A physical prototype was developed to test this linear motor, and other key technologies were identified to solve the problems of the system. This thesis demonstrates the feasibility of this linear engine, and presents a preliminary design.

Acknowledgements

In a fast German car,
I'm amazed that I survived,
an airbag saved my life.
-Radiohead

There were many individuals and groups without whom it would not have been possible to complete this thesis. This work stands as a tribute to their generous support.

First, I am thankful to the National Science Foundation for providing me with a Graduate Research Fellowship during the past three years. I must also express my gratitude to the Stanford University School of Engineering, which provided fellowship support during my first year and supplemented the NSF funds. The value of versatile and open ended funding is clear to a creative research program. My advisor and Prof. Tom Kenny at Stanford, as well as Prof. K.T. Ramesh and Prof. Louis Whitcomb at Johns Hopkins deserve special credit for their wise council in securing these fellowships.

Next, it is incumbent upon me to acknowledge the faculty of the Mechanical Engineering Department and sundry Control Systems faculty at Stanford. Their pedagogy allowed me to gather the necessary skills to address advanced research topics. Worthy of particular praise are Prof. Ed Carryer for the unique and magnificent Smart

Product Design course series, and Prof. Stephen Boyd for his witty, insightful classes on dynamic systems. Of less direct value to my research was Prof. Bernie Roth's class "The Designer in Society", which nonetheless was in itself an education hard to parallel in the academic world.

Many friends have been here to provide me with emotional support and an escape from daily tedium. The one, the only, the truly incomparable Leland Stanford Junior University Marching Band deserves accolades as an organization in this capacity. I wish I could thank each of its members, but especially Joey Bravo, Joel Knudsen, and Ringo Riley. Others outside of the lab who helped keep me sane include Shelley Fairweather, who writes me letters from Italy, Seattle, and Russia, Patrick Owens, who always reminds me when I forget that the world is full of stupid people, and Mez Polad and Jen Doran, who allowed me the joy of participating in a Zoroastrian-Catholic wedding.

In fall of 2000, I spent one day a week at Sandia National Labs, in order to learn about their ongoing linear engine project. This experience was immensely useful, and Nick Paradiso, Scott Goldsborough, and Peter Van Blarigan at SNL have my thanks.

Several people associated with the Engine Lab were of great help to me. Pat Caton provided me with data from his HCCI experiments and advice on engine modeling. A.J. Simon provided more of the same, and a great deal of useful advice on the design of the linear engine. Scott Sutton was a constant source of information on manufacturing techniques and engine design.

The most important contributor from this side was Prof. Chris Edwards, who served as my co-advisor on this project. His knowledge of engines is surpassed only by his passion for the subject. Whenever I talked with him, he was always ready with useful answers and words of encouragement. Without his support, I could not have begun to address the thermodynamic and engine design issues so central to this research.

The Dynamic Design Lab has hosted me for nearly four years now, and interacting with its members has been one of the most rewarding parts of my research experience. Many of my problems were solved by my peers, who always seemed to have time to listen. Most important of these were Eric Rossetter, who was good enough to inadvisably trust me with his life while driving down Page Mill Road, and Chris Carlson, who even put up with living with me. Other important sounding boards and compatriots were Greg Shaver, Matt Schwall, Sam Chang, Jihan Ryu, and Paul Yih. Hong Bae deserves my particular thanks for educating me about the process of writing an Engineer's Thesis. Special recognition goes to Doug Bourne, who during summer of 2001, worked with me on this project. His contribution is difficult to overestimate, both in terms of his actual work output and as a sounding board.

No one was more instrumental in this process than my advisor, Prof. Chris Gerdes. During my time at Stanford I was pleased to work with him as he made the transition from industry wizened newcomer to a professor emblematic of Frederick Terman's idea of a "steeple of excellence". He was resourceful and supportive in coming up with funding for this research, and patiently guided the process through many apparent dead ends. I've learned a great deal about engineering from him, and he helped me to learn much about myself.

Finally, I must thank my family. My brothers, Paul and Tom, have always been my best friends, and help me to keep things in perspective. My father, Ronald, is my most important role model as an engineer and as a good sport. My mother, Diana, taught me most of what I know about being a decent person. This thesis is devoted to them.

Contents

List of Tables

List of Figures

Chapter 1

Introduction

This thesis documents the development of an unusual form of internal combustion engine as an experimental research apparatus. In this engine the crankshaft, which translates linear motion into rotary motion, is replaced by a linear electrical machine, which transforms linear motion into electrical power. The development is advanced to the point of demonstrating feasibility by simulation, prototyping, and the exploration of enabling technologies.

This work was carried out between 2000 and 2002 in the Department of Mechanical Engineering at Stanford University. Most of the work was performed by the author, under the supervision of Prof. Chris Gerdes, the Principal Investigator. Prof. Chris Edwards also had a significant advisory role. Doug Bourne spent a summer working on this project for an undergraduate research experience, and much of the work towards specifying components (especially the optical encoder, the cables, the bearings, and the shock absorber) was his.

This thesis is organized as a design document. The first chapter sets the work in context, by describing the ubiquity and importance of the internal combustion engine, and its application to electrical power generation by coupling it with an electrical machine. Then, the concept of the linear engine, where the crankshaft is replaced by a linear electrical machine, is introduced. Finally, it is stated that this thesis solves the problem of developing a linear engine to the point of feasibility.

In the second chapter, research in linear engines at West Virginia University, Sandia National Labs, and the University of Regina is reviewed for the purposes of benchmarking. A set of priorities was determined, which led to requirements that the engine employ a four stroke working cycle, feature a single unopposed piston, and be built on the same scale as existing research engines.

In the third chapter, thermodynamic, electrical, and dynamic models are integrated to implement a simulation of the linear engine in Matlab Simulink. Based on this simulation, a linear electric motor, the Aerotech BLMX-502b, was selected as the electrical machine. A prototype was built to test the linear motor.

The fourth chapter describes the selection of components to solve the problems of constraining the piston to linear motion, stopping the piston in case of a failure, and connecting the moving assembly electrically. Then a possible mechanical design for the overall system is presented.

The fifth chapter demonstrates how the work described in the previous chapters establishes feasibility and suggests directions for future work.

1.1 Context

1.1.1 Historical Perspective

The internal combustion engine was first realized in its modern form by Nikolaus Otto in 1867 [13, 20]. The technology spread quickly, and by World War I, the internal combustion engine was ubiquitous in both mobile and stationary applications.

With the advent of mass production, automobiles actuated by this chemical power plant entered the garages of middle class America. Around the world, fortunes were made and lost by those who made automobiles, fuels, tires, and all the other things necessary for peoples' new found mobility. By the 1940's, cities like Los Angeles were transformed by new patterns of housing, labor, and even climate due to the automobile. Meanwhile, the internal combustion engine had found applications in airplanes and sea going vessels. In manufacturing and power generation, these sources of mechanical energy were also common.

Today, internal combustion engines are everywhere, and there are growing social concerns surrounding their emissions, the procurement of their fuels, and their production. Some suggest that their utility for many applications will end. However, it is clear that, for the moment, there are many applications where no other technology will be practical for some time. Therefore, research into improving the internal combustion engine is still of great social and economic importance.

1.1.2 Classification of Internal Combustion Engines

There are many ways in which internal combustion engines may be classified [13, 6]. However, if we limit the scope to geometries involving reciprocating pistons (as opposed to rotary or Wankel engines), two broad distinctions are of special importance.

The first is the number of strokes the piston moves through to complete a full engine cycle. Virtually all automotive applications are four stroke designs. An idealized thermodynamic representation of this working cycle for gasoline engines, in terms of the pressure and volume of the combustion chamber, is shown in fig. 1.1.

According to this design, air, or an air/fuel mixture, is inducted in the first stroke, Intake. Following this, the volume of the combustion chamber is reduced, compressing the gases. At the end of the Compression stroke, near the minimum volume, the charge ignites, releasing energy. During Expansion, the combustion chamber increases in volume, converting heat energy into mechanical work. Finally, the products are expelled during the Exhaust stroke.

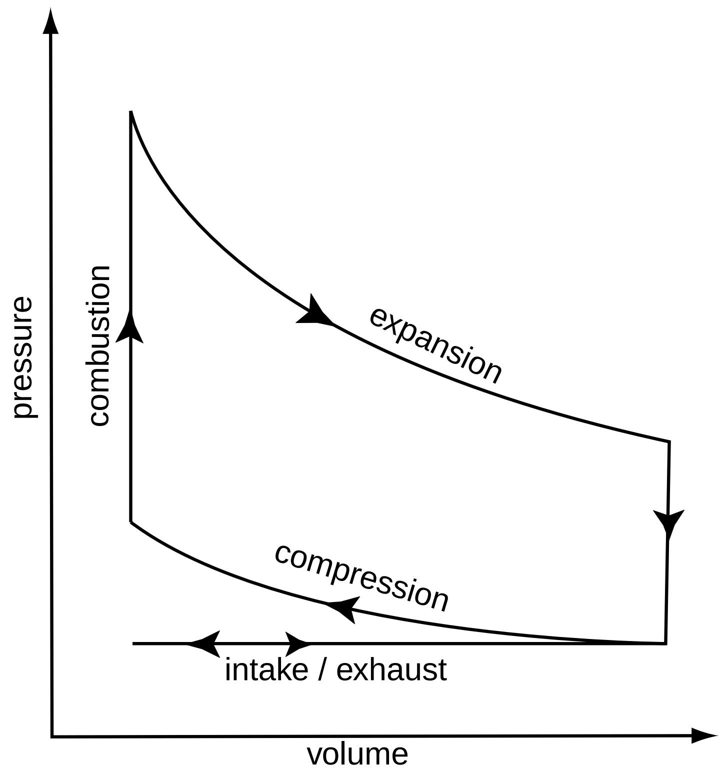

Figure 1.1: Ideal Otto Cycle

More common in small and very large internal combustion engines is the two stroke working cycle. This design is similar to the four stroke cycle, except that the induction and exhaust processes occur during the transition between the Expansion and Compression strokes, rather than during separate strokes.

This usually necessitates that induction and exhaust occur simultaneously through a process called scavenging. While there are ways to implement extremely effective scavenging, in the low weight, low cost applications in which small two strokes are typically applied, scavenging often results in wasted fuel and poor efficiency. Two stroke engines, however, enjoy a significant advantage over four stroke engines in power to weight ratios, due to the fact that they have twice as many power strokes per engine revolution.

The other major distinction to be made in classifying engine types is the manner in which the charge is ignited. In most gasoline engines, an electric spark is used to initiate combustion. A flame front starts near the spark, and propagates until the fuel is consumed. These engines can have good power to weight ratios, but their efficiency is limited by the maximum cylinder pressure, which must be kept below the threshold of autoignition during compression. Also, since torque is typically regulated by throttling the air intake, efficiency is further reduced during part load operation.

Diesel engines, however, utilize compression ignition. Because combustion is more easily initiated in this fuel, it is possible to start the combustion process at moderate cylinder pressures without a spark. Usually, in order to precisely control the timing and amount of fuel combusted, the fuel is sprayed into the combustion chamber via direct injection. These engines are often heavier and bulkier than spark ignition engines, but they are also generally more efficient due to their higher compression ratio and lower pumping losses.

1.1.3 Engine Components

While internal combustion engines vary significantly in shape, size, and function, if one considers the important case of 4-stroke, spark ignition engines, there are a handful of elements common to most designs (see fig. 1.2.)

The piston moves up and down, allowing the sealed combustion chamber to change in volume. The valves open in coordination with this motion to allow gases in and out. When the charge is ready, a small region of plasma is created by the spark plug in order to initiate combustion.

The crankshaft, along with the connecting rod, converts the reciprocating linear motion of the piston into steady rotary motion. The crankshaft typically has a large amount of inertia, and thus only changes rotational velocity gradually (significant changes only occur over the course of many engine cycles.)

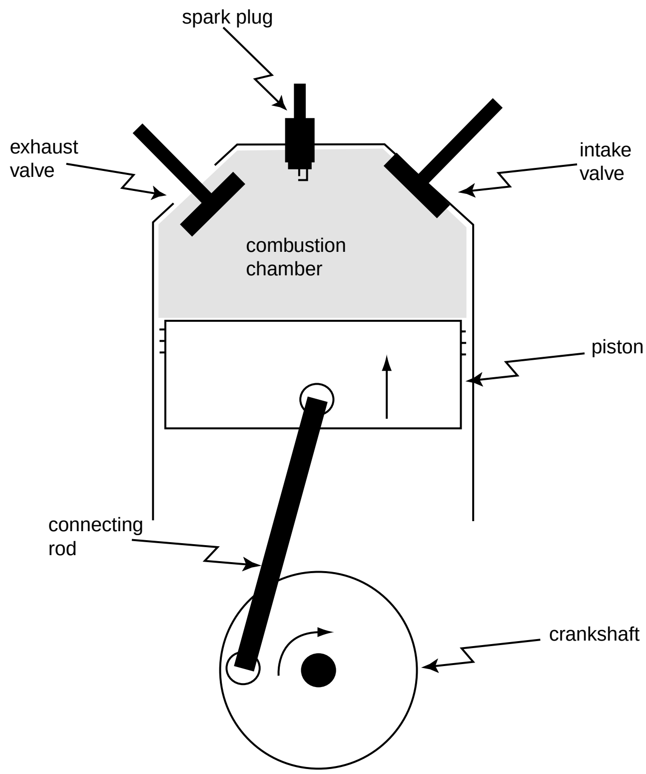

Figure 1.2: Schematic Engine

1.1.4 Generation and Electrical Machines

Many I.C. engines are used to generate electrical power for such applications as electricity in remote locations, supplying specialized electrical motors (as in hybrid electric vehicles) and emergency power. In order to accomplish this, the engine must be coupled to an electrical machine.

Electrical machines convert mechanical energy to electrical energy, or vice versa. It is feasible to build them in a variety of geometries, such as rotary or linear, and, given appropriate power control circuitry, it is feasible to operate them under steady or time varying conditions. Most electrical machines consist of two major parts: a stationary assembly, called the stator, and a moving assembly, referred to as the rotor (regardless of whether its motion is actually rotary.) A back iron, usually consisting of laminated ferrous sheets, is sometimes used to modify the behavior of the magnetic fields. Resistive losses, which result in the dissipation of electrical energy as heat, are significant factors in the efficiency of these machines.

Typically, when using an I.C. engine to generate electrical power, a rotary electrical machine is coupled to the crankshaft, and the system is designed to operate under steady conditions.

1.2 Need Statement

If an engine is used solely to produce electrical power, it is not necessary to convert the reciprocating linear motion of the piston to steady rotary motion. Instead, a linear electrical machine may be coupled directly to the piston.

Such a design would open a large unexplored design space. From a machine design stand point, there are opportunities to use fewer parts and improve reliability. Because the lateral forces imposed by the crankshaft are eliminated, there are opportunities to reduce friction and achieve better sealing.

From a thermodynamic standpoint, the opportunities are even more far reaching. The piston is uncoupled from the inertia of the crankshaft, and the electrical machine may be controlled to allow for an essentially arbitrary piston position time history.

This could allow improvements to cycle efficiency such as by implementing the Atkinson cycle. The Atkinson cycle improves on the Otto cycle by delaying the opening of the exhaust valve until the pressure in the combustion chamber is near ambient (see fig. 1.3). This extracts more work from the gases, but requires a stroke which is longer during expansion and exhaust than during intake and compression.

It could also allow for novel combustion strategies such as Homogenous Charge Compression Ignition. This strategy allows gasoline engines to utilize compression ignition part of the time. Via preheating of the intake gases, intentionally retaining or

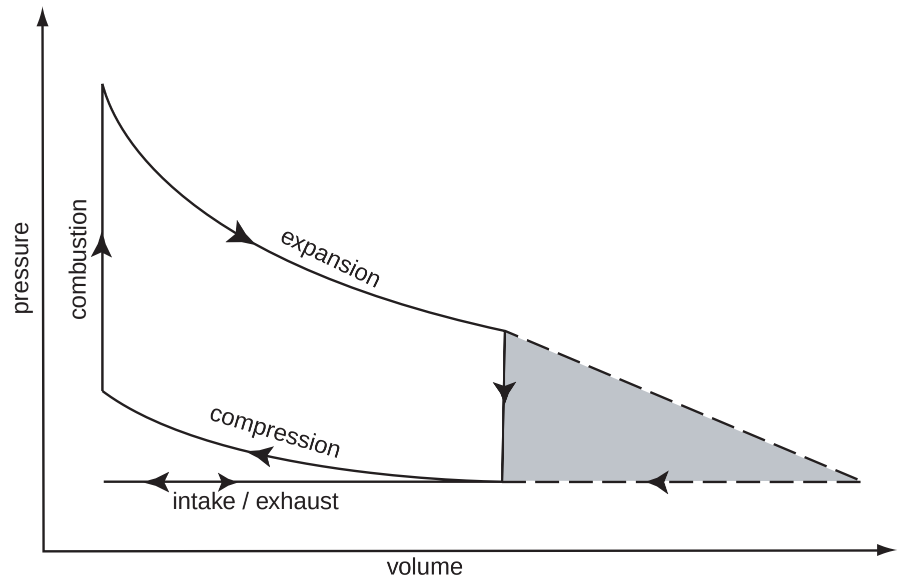

Figure 1.3: Ideal Atkinson Cycle

reinducting exhaust residual, or, in this case, by changing to a high compression ratio, the charge undergoes a very rapid compression ignition. Under certain operating conditions, this strategy has been demonstrated to improve efficiency and reduce emissions [14, 21].

1.3 Problem Statement

Such a device, in which the crankshaft has been replaced by a linear electrical machine, could be referred to as a linear engine (see fig. 1.4.) This thesis will solve the problem of developing the design of a linear engine to the point of demonstrating feasibility.

In the long term, this engine could be used in such applications as home power generation or hybrid electric vehicles. However, even if these applications do not prove commercially viable, the linear engine will have great immediate value as a laboratory tool to explore the design of internal combustion engines.

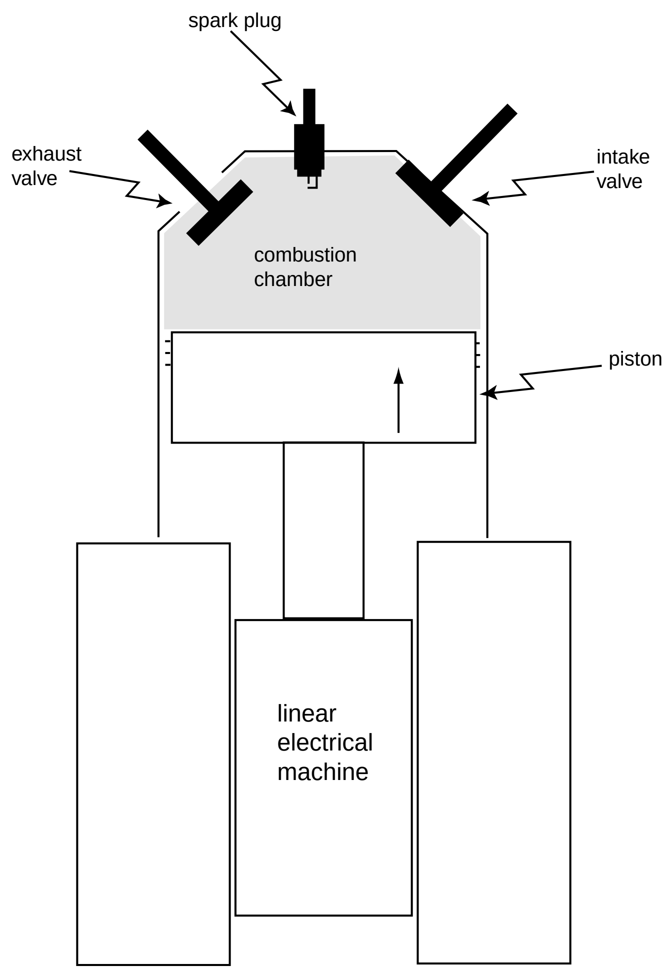

Figure 1.4: Linear Engine

Chapter 2

Design Requirements

After establishing the problem that the research would solve, requirements were defined for the design. Linear engines for electrical power generation have been investigated recently by groups at West Virginia University, Sandia National Labs, and University of Regina, so their work was reviewed for benchmarking purposes. Based on the lessons learned from the work of others, representatives from the Gerdes and Edwards research groups agreed upon a set of priorities, which emphasized the linear engine's role as an effective research apparatus and as a test bed for new technologies. Based on these priorities, a set of requirements was defined, specifying that the linear engine should operate with a four stroke working cycle, that it should consist of a single piston, and that it should be of comparable scale to existing research engines.

2.1 Benchmarking

Benchmarking was undertaken to determine the state of the art and repeat the good practices of others, as well as react to the bad practices. These lessons were applied through the requirements definition and the rest of the design process.

A concept related to the linear engine is the free piston engine. Free piston engines

Group	Bore(mm)	Stroke(mm)	Reciprocation Rate (cycles/min)	Power (kW)
WVU	36.5	50	1460	0.30
SNL	70.0	164	3000	30.00
Regina	30.5	27	2000	0.29

Table 2.1: Summary of Benchmark Linear Engine Parameters

have one or more pistons which are not constrained by a crankshaft. These pistons are typically coupled to a fluid system. In the 1950's, two stroke, spark ignition free piston engines were used to produce hot gases to drive a turbine [9]. It was hoped that the turbine could serve as an automotive power plant, but it proved too expensive and inefficient in this setting. Free piston engines have enjoyed wider use as a means to pump and compress fluids [1]. One particularly interesting aspect of these engines is that they often employ pulse pause operation, where power output is modulated by pausing the piston at the end of each cycle.

Most of the work on linear engines for electrical power generation has been carried out in the 1990's, enabled by developments in power control and linear electrical machines. The most important published work in the field has come from teams at West Virginia University, Sandia National Labs, and the University of Regina. A summary of important parameters for each of these engines is shown in table 2.1.

2.1.1 West Virginia University

Since the late 1990's, Prof. Parviz Famouri at West Virginia University (WVU) has led an effort to develop a linear engine. To date, this effort is probably the most successful realization of the linear engine as source of electric power.

As Clark et al explain [5], the system is based on a pair of opposed cylinders, operating under a two stroke working cycle. Combustion is initiated with an electric spark, and the incoming charge is propelled with house air. With this arrangement, one of the two cylinders is in the power stroke at all times, so the thermodynamic system requires no other energy input except for starting. The engine was first realized with no electrical machine. The piston body was allowed to reciprocate without an external load, dissipating most of the fuel energy through waste heat and friction. Pistons were adapted from a Homelite chainsaw, yielding a bore of 36.5mm, with a maximum possible stroke of 50mm. This reuse of stock parts saved significant effort in designing and fabricating pistons for effective scavenging, and serves as a good design lesson for other linear engines. Under no load, reciprocation rates of 1457 cycles/minute were obtained.

Famouri et al [7] detail the design and testing of a linear alternator for the engine. Based on a design approach put forth by Boldea and Nasar [3, 4], this alternator features moving magnets in a ring formation located concentrically within a series of static coils. The opposed cylinder design means that the electrical machine never has to function as a motor, simplifying power control considerably. Using a resistive load, the experimenters were able to achieve an output power of over 300W before stalling the engine.

Atkinson et al [2] describe the development of a numerical model of the linear engine. This analysis breaks down the cycle into distinct processes, and applies a single zone thermodynamic model to each of them. The model was validated with experimental results. The engine was simulated subject to a series of position varying load profiles, which yielded significant variations in peak pressure. This suggests the promise of using the electrical machine as a means of influencing combustion with a control system.

2.1.2 Sandia National Labs

Another group, under the supervision of Dr. Peter Van Blarigan at Sandia National Laboratories (SNL) in Livermore, California has been developing another linear engine in the 30kW range. This engine is similar to the WVU design in that it has two opposed cylinders operating in a two stroke working cycle. However, the SNL efforts differ in that they utilize Homogenous Charge Compression Ignition, with a variety of fuels.

The first investigation, as elucidated by Van Blarigan et al [21], was a series of experiments using a Rapid Compression Expansion Machine (RCEM.) In this device, a charge is placed in a cylinder, and allowed to reach a quiescent state. A reservoir of helium gas is pumped to a pressure of about 50 MPa. This gas is then rapidly deployed to move the piston, thus compressing the charge. Compression ratios of 30:1 are typical, resulting in autoignition of most common fuels. This experiment was intended to show the advantages of nearly constant volume combustion at high compression ratio. Blarigan et al claim cycle thermal efficiency of up to 56% using this technique.

Goldsborough et al [11] describe a numerical study of the linear engine in development at SNL. A one dimensional thermodynamic model is applied, as is the case with the WVU simulation. However, because the SNL team is more concerned with fuels, efficiency, and emissions, a detailed chemical kinetic model was implemented using HCT software developed by Lawrence Livermore National Laboratory. The engine has a bore of 70mm and a typical stroke of 164mm. In simulation, using hydrogen as a fuel, Goldsborough et al claim indicated ideal cycle thermal efficiencies of near 65%, with reduced NO_x emissions. The authors note that actual performance will be extremely dependent on the implementation of the scavenging process.

While the cited efficiency numbers are optimistic for most applications, based as they are on extremely high compression ratios (30:1) and ideal laboratory conditions in the case of the RCEM, HCCI is certainly a promising technology for use in a linear engine. Another important lesson from the Sandia project is that producing a custom electrical machine can be a major investment; the development so far has necessitated complicated analytical software, the involvement of an outside contractor, and exploration of unusual fabrication techniques.

2.1.3 Kos and University of Regina

In 1991, Joseph F. Kos was granted a patent [15] which covers linear engines for electrical power generation. The patent specifically describes arrangements with a single cylinder and with two opposing cylinders. The patent also makes reference to the ability to use computer control to improve performance.

A team at the University of Regina set out to investigate the potential of the linear engine, using Kos's invention as a starting point. Zhang, as part of his Master's thesis [24], describes the modeling and simulation of this engine. These simulations considered the case of a single cylinder opposed by a linear motor/generator along with a spring, which stored energy at the bottom of the stroke. A case with two opposed pistons was also considered.

The simulated engine had a bore of 30.5mm and a stroke of 26.7mm. A two stroke working cycle was used, and no means of ignition is explicitly stated. The thermodynamic model is based on a single zone, with instantaneous heat addition occurring at top dead center. Peak power output of 290W for the unopposed case was reported. The simulated electrical machine powered a range of resistive loads, and the best power output occurred when the ratio of internal resistance to external resistance was 1:2. The main lesson from this work was that a spring may be used effectively with a single cylinder design to reduce the load on the electrical machine.

2.2 Requirements Definition

After the process of benchmarking, requirements were defined for the design by discussion among the Gerdes and Edwards research groups. Based on research objectives and practical limitations on resources, a consensus was reached on a set of priorities for the linear engine. These priorities guided the process of defining specific requirements.

The first priority was that the engine be an effective research apparatus. This efficacy can be measured by the sorts of experiments which may be carried out with the device. The experiments deemed most important involved investigating different combustion regimes, with a control system to manage them. This necessitates a broad range of possible strokes, a strong ability to affect the piston motion via actuation, the ability to sense data in real time, and control over the mass exchange processes.

The second priority was to investigate technologies which could be applied not only to this application, but also to other research important to the labs involved. Linear electrical machines can be applied to variable valve actuators, to fuel injectors in continuous combustors, and to test apparatus for vehicle dynamics. The linear engine will pose design opportunities in bearings and sealing, due to its absence of side forces. Finally, solving the power control needs of such a system will suggest other applications.

A lesser priority was to develop a practical machine for electrical power generation. While this would be a desirable outcome, it was decided that it would compromise the first two priorities too much to make it more important. Additionally, the other teams have already addressed this problem in some depth, and it was deemed more important to examine other directions.

Given these priorities, it was not difficult to make decisions about the requirements. The major categories of requirements concerned the working cycle, the configuration, and the scale of the linear engine.

2.2.1 Working Cycle

Internal combustion engines are typically either four stroke or two stroke. Two stroke engines make more power per unit displacement, and for some applications may be mechanically simpler. When designing a scavenging system, either careful attention must be paid to the details of the fluid system, or poor performance must be tolerated. For the purposes of a research apparatus, either of these options reduces the experimental utility of the system.

Four stroke engines produce less power per cycle. However, because the intake and exhaust processes occur independently over the course of separate cycles, it is easy to design a poppet valve system to effect good mass transfer. A variety of special strategies can be applied, such as valve throttling and residual reintake. Therefore, the linear engine should use a four stroke working cycle.

2.2.2 Configuration

As is the case with working cycle, two alternative configurations were worth considering: a single cylinder, or some arrangement of opposed cylinders. Other configurations may be possible, but most would circumvent the advantages of eliminating the crankshaft.

The consensus was not to make an opposed piston design a requirement for several reasons. First, the single cylinder is mechanically simpler. It is only necessary to provide one piston and one apparatus for mass exchange. These elements would have to be duplicated in an opposed design. Second, while the opposed piston enjoys an advantage with a two stroke design in that it never requires energy input from the electrical machine to run, with the four stroke design this advantage may only be realized with four cylinders. This would complicate the design significantly. Lastly, with the opposed piston design, the pistons would be coupled, and thus their positions could not be varied independently. This would mean that one could not change the position time history of one stroke without affecting another on the opposite cylinder.

Given the decision that the linear engine should use a single, unopposed piston, it is possible to improve the performance of the system by including other devices.

In particular, by adding some kind of spring which would come into play as the piston reached bottom dead center, it would be possible to mechanically store some of the energy of the piston's down stroke and restore it on the upstroke. Because electrical machines tend to have poor efficiency near stall conditions, this spring could lighten the load on the actuator, and improve system efficiency. However, a spring which would exhibit enough flexibility to serve this role under a variety of operating conditions would be difficult to implement, and could add significant complexity to the system. Because experimental utility, and not efficiency, was our highest priority, the stake holders decided not to require a spring, at least for the first generation linear engine. It may be worthwhile to reconsider this decision for future implementations.

2.2.3 Scale

The linear engine could be realized in many sizes. The efforts surveyed above range from hundreds of Watts to 30kW, and a patent exists for a MEMS-based linear engine [10]. At the small end of scale, one is limited by the ability to fabricate precise parts, obtain small actuators and sensors, and by thermodynamic relations affected by square-cube relations (for example, heat loss is related to the ratio between the volume of the combustion chamber and its surface area.) At the large end, the primary limit is cost. The deciding factor was interfacing with existing equipment. Two existing apparati presented special opportunities to ease the realization of the linear engine, and a decision was made to require that the linear engine interface with them.

The first is the optical cylinder. This is an experimental device designed to allow optical access to a combustion chamber. This is executed with the aid of a crystal cylinder, usually made of quartz or synthetic sapphire. The optical cylinder allows lasers to be passed through the combustion gases, yielding information about their state. Because the cylinder is brittle, it is necessary to use a hydraulic clamping device to secure it in place. If necessary, a steel tube may replace the crystal cylinder for longer duration tests.

The second is the Variable Valve Actuation (VVA) system. This is an electrohydraulic system (see fig. 2.1) which can open and close intake and exhaust valves at arbitrary times in the engine cycle. The elimination of the crankshaft in the linear engine also means the elimination of the camshaft; VVA fills this void well and adds functionality.

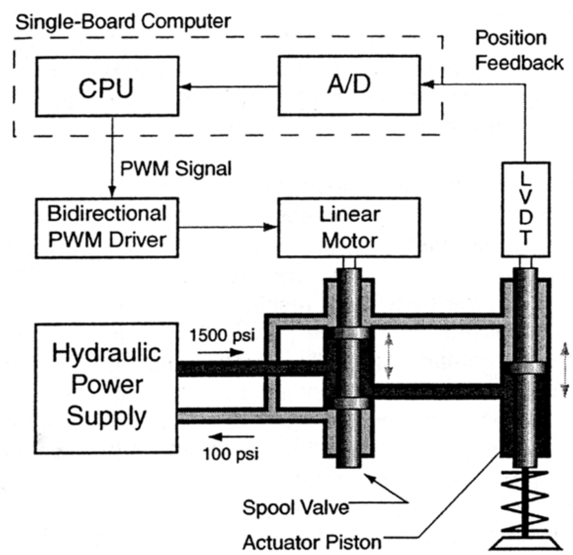

Figure 2.1: Schematic of Variable Valve Actuation System (taken from [14] with permission)

Together, the VVA and the optical cylinder solve many problems of developing a linear engine. They are also designed to be applied to a traditional crankshaft, so cross comparisons could be made of the optical engine/VVA in the linear and traditional configurations. Because the VVA is designed to attach directly to the top of the optical engine, it is only necessary to design around the interface with the optical engine. The interface occurs on a plane, and has the layout shown in fig. 2.2.

In addition to attaching to this surface, the linear engine must conform to the

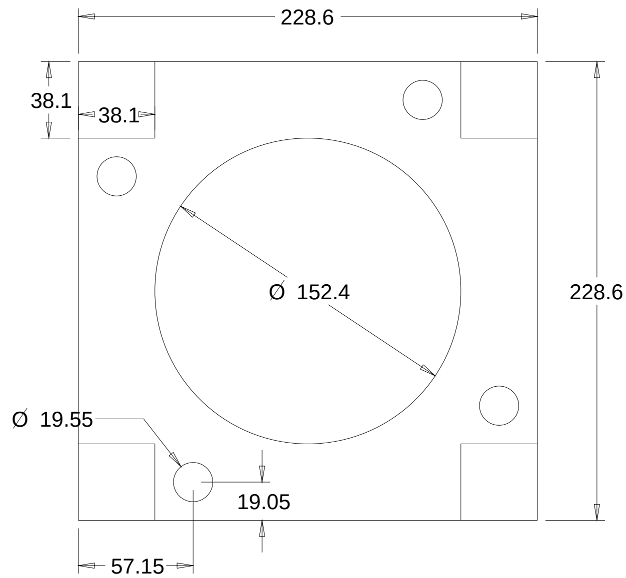

Figure 2.2: Optical Cylinder Interface

bore of the optical cylinder, which is 92mm, and the stroke, which is near 100mm. In order to compare data between the linear and conventional engine, the linear engine should also be able to achieve a reciprocation rate of 800-1000 cycles per minute.

Finally, by working in the power range appropriate to these dimensions (several kW,) it is possible to use commercially available electrical machines. Based on the some of the difficulties other groups have experienced in developing a custom electrical machine, and the desire to get a prototype working relatively quickly, the linear engine should use a stock electrical machine.

Chapter 3

Design Development

The general framework for the linear engine was established by the requirements that it use a four stroke working cycle, that it employ a single piston, and that it be of comparable scale to existing research engines. Based on this framework, it was now possible to begin to develop the design. The first stage in this development was to implement a model of the linear engine system in Matlab Simulink. A single zone thermodynamic model was integrated with a static model of the electrical machine and the mechanical dynamics. The PV diagram produced by this model was adjusted to resemble the experimental PV diagram of an existing research engine. With these results, it was possible to determine specifications for an ideal electrical machine. A survey of electrical machines suggested that no available technology could meet these specifications at a reasonable cost, but that the Aerotech BLMX-502b brushless DC linear electric motor could come close to achieving the ideal motion profile within the project budget. Because the linear motor was a key enabling technology for the linear engine, a prototype was constructed to confirm its operation and to explore design implementations. A test of the motor constant was conducted which measured results similar to Aerotech's specification at moderate motor forces (10%-15% rated peak load), but which exhibited some unexpected behavior at a low load (5% peak) which may require compensation.

3.1 Modeling

The primary motivation for modeling was to gain a better understanding of the system. Additionally, modeling was necessary in order to select and test the electrical machine, to determine forces for mechanical design, to estimate the breadth of the experimental utility of the system, and to design a controller for the engine. In order to develop the model, the thermodynamic system was analyzed first, then the electrical machine was added. Finally, these aspects were integrated with the mechanical dynamics and implemented in Matlab Simulink.

3.1.1 Thermodynamic System

Model Scope

Internal combustion engines may be modeled at many levels [8, 6, 13, 20]. For the most demanding applications, finite element models accounting for thermodynamic effects, fluid dynamics, chemical kinetics, and heat transfer at the the detail level may be implemented. At the other end of the spectrum, for analyzing applications such as cruise control, it may suffice to address engine modeling in terms of average mass flow. Most models will lie between these extremes, with complexity commensurate to the requirements of the task.

For the purposes of the linear engine, the main requirement of the thermodynamic model was that it represent the magnitude and general time evolution of the pressure in the combustion chamber in order to determine the force on the piston. Because the model was based on an engine design which already had experimental data from the

Variable	Description
x	position
p	pressure (Pa)
V	volume (m^3)
m	mass (kg)
R	gas constant ($\frac{J}{kg \cdot K}$)
T	temperature (K)
U	internal energy (J)
u	specific internal energy (J/kg)
c_v	constant volume specific heat ($\frac{J}{kg \cdot K}$)
Q	heat (J)
$\dot{Q}$	heat flow (J/s)
$\dot{W}$	work input (J/s)
$\dot{h}$	specific enthalpy flow
γ	ratio of specific heats
a	empirical constant
b	empirical constant
t	time (s)
t_s	time combustion starts (s)
t_c	duration of combustion (s)
C_D	coefficient of drag
A_R	reference area (m^2)
p_T	downstream pressure (Pa)
p_0	upstream stagnation pressure (Pa)
T_0	upstream stagnation temperature (K)
$p_{manifold}$	manifold pressure (Pa)
p_{piston}	piston pressure (Pa)
c_1	empirical constant ($\frac{kg}{s \cdot Pa}$)
F	force (N)
q	charge (C)
B	magnetic flux density (T)
L	length of wire (m)
n	number of coils
I	current (A)
v	velocity (m/s)
θ	angle (rad)
k_m	motor constant ($\frac{N \cdot s}{C}$)
w	work (Nm)
ε	back EMF (V)
V_{term}	terminal voltage (V)

Table 3.1: Notations for Modeling

HCCI experiments [14], it was not necessary for it to predict all combustion parameters. According to these conditions, a single zone model, with empirical relations for fuel energy release and a simple approximation for mass transfer, was applied.

Derivation

The thermodynamics of this model may be derived from first principles, given a few assumptions. First, one must assume that the ideal gas law,

$$pV = mRT \tag{3.1}$$

holds. Second, one must assume that ideal gas parameters R and γ, under the conditions of the combustion chamber, may be approximated as constant. Also, one must assume that the specific internal energy u is a function only of temperature. For the purposes of this model, a first order relation corresponding to a constant specific heat was reasonable:

$$\frac{du}{dT} = c_v \tag{3.2}$$

Finally, it is assumed that it is reasonable to approximate the contents of the cylinder as a single species, with constant gas parameters chosen to approximate the aggregate behavior of the multiple species actually present. These assumptions represent convenient approximations, which do limit the ability of the model to represent complex engine phenomena, especially spatial variations in temperature and pressure, and emissions. However, these assumptions do allow enough richness in the model dynamics to represent the general shape of the pressure curve.

With these assumptions established, we may derive our model starting with the First Law of Thermodynamics:

$$\frac{d}{dt}U = \dot{Q} - \dot{W} + \sum_{j=1} \dot{m}_j h_j \tag{3.3}$$

For the single zone model, with enthalpy flow due entirely to the valves:

$$\frac{d}{dt}U = \dot{Q} - p\dot{V} + \dot{m}_{int}h_{int} + \dot{m}_{exh}h_{exh} \tag{3.4}$$

Due to equation 3.2,

$$\frac{d}{dt}U = \dot{m}c_v T + mc_v\dot{T} \tag{3.5}$$

and we may derive:

$$\dot{T} = -\frac{T\dot{m}}{m} + \frac{1}{mc_v}(\dot{Q} - p\dot{V} + \dot{m}_{int}h_{int} + \dot{m}_{exh}h_{exh}) \tag{3.6}$$

Based on the ideal gas law:

$$\dot{p} = \frac{RT}{V}\dot{m} + \frac{mR}{V}\dot{T} - \frac{p}{V}\dot{V} \tag{3.7}$$

Using the relation,

$$\gamma - 1 = \frac{R}{c_v} \tag{3.8}$$

and substituting equation 3.6 in to equation 3.7, we may derive the expression:

$$\dot{p} = -\frac{\gamma p}{V}\dot{V} + \frac{\gamma - 1}{V}\left(\dot{Q} + \dot{m}_{int}h_{int} + \dot{m}_{exh}h_{exh}\right) \tag{3.9}$$

This differential equation is the basis for the model, but in order to solve it, we must address mass exchange and heat transfer. The energy release due to combustion is modeled as heat transfer with a time based Wiebe function [20, 2]:

$$\dot{Q}_{fuel} = Q_{fuel_{total}} a\frac{b+1}{t_c}\left(\frac{t-t_s}{t_c}\right)^b exp\left[-a\left(\frac{t-t_s}{t_c}\right)^{b+1}\right] \tag{3.10}$$

with combustion modeled to begin at a specified time near the end of the compression cycle. This model would be appropriate to either spark ignition or compression ignition. Aside from the heat addition due to fuel, the cylinder is considered to be adiabatic. Mass transfer is addressed by assuming there is no leakage through the piston rings, and invoking conservation of mass:

$$\dot{m} = \dot{m}_{int} + \dot{m}_{exh} \tag{3.11}$$

Finally, considering the mass flow through each valve, Heywood [13] describes the following relation :

$$\dot{m} = \frac{C_D A_R p_0}{\sqrt{RT_0}} \left(\frac{p_T}{p_0}\right)^{\frac{1}{\gamma}} \sqrt{\frac{2\gamma}{\gamma - 1}\left[1 - \left(\frac{p_T}{p_0}\right)^{\frac{\gamma-1}{\gamma}}\right]} \tag{3.12}$$

This rather complicated expression may be computed from first principles by examining compressible flow through a flow restriction. It models flow through a poppet valve well, and was the initial choice for the linear engine model. However, this expression proved numerically problematic when an ODE solver was applied to the system, due its behavior when $\Delta p = (p_{manifold} - p_{piston})$ crosses zero. A much simpler expression,

$$\dot{m} \approx c_1 \Delta p \tag{3.13}$$

proved adequate for modeling the deviations in pressure due to pumping fluid through the valves, which were much smaller than the pressure changes during the compression and expansion processes, yielding a qualitatively similar PV diagram for the two expressions for mass flow. However, it should be noted that this simplification was only reasonable because of system dynamics specific to this model of engine behavior, and is not in general guaranteed to yield good results.

3.1.2 Linear Electrical Machine

There are varied approaches to modeling of electrical machines as well. However, in general, they are easier to model than combustion systems since they typically involve only a few moving bodies (as opposed to a continuum of fluid) subject to magnetic and electrical fields, which although continuously variable over a three dimensional space, have much simpler dynamics than fluid systems. However, the detailed finite element models which would provide the best accuracy are still computationally intensive and difficult to analyze. For the purposes of modeling the linear engine, a simple static representation based on physical principles is a reasonable approximation [24, 16, 12].

The relevant physical principles relate to the forces on an electron in a magnetic field, as described by Lorentz's Law:

$$F = q(\vec{E} + \vec{v} \times \vec{B}) \tag{3.14}$$

Along a length of wire with a steady current located in a uniform magnetic field (see fig. 3.1), one may derive the following expression:

$$F = BLI \sin\theta \tag{3.15}$$

If one were to wrap this wire into a solenoid (see fig. 3.2), with a number of turns oriented such that the current flow is perpendicular to the magnetic field, the following equation would result:

$$F = nBLI \tag{3.16}$$

This solenoid is actually fairly close to the typical design of an electrical machine. Considering a configuration similar to the solenoid, but with additional elements in order to optimize the magnetic circuit, the effects of which could be derived or

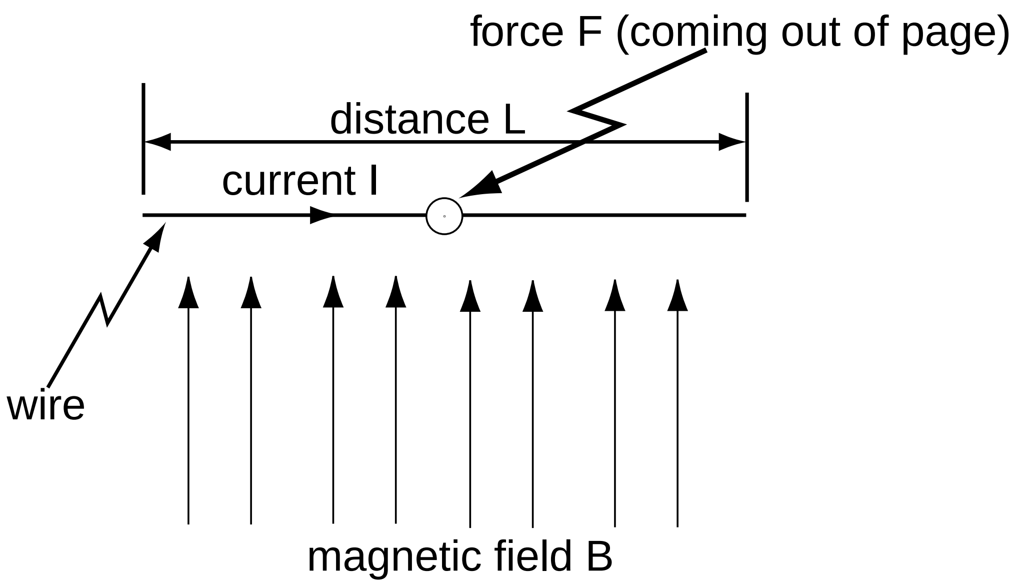

Figure 3.1: Wire in a Magnetic Field

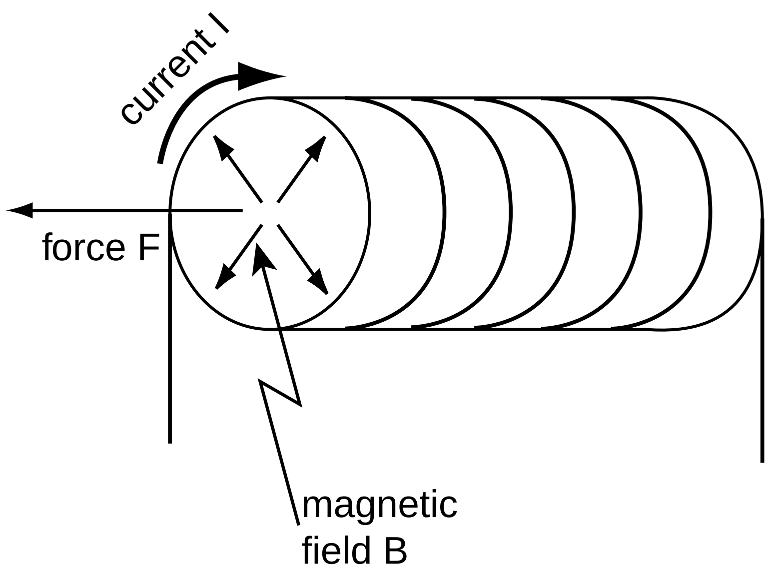

Figure 3.2: Solenoid

measured in an aggregate sense, we arrive at the first major equation necessary to model the electrical machine:

$$F = k_m I \tag{3.17}$$

In reality, the relationship between current and force does exhibit some dynamic behavior, and is somewhat nonlinear even when considered in a static sense. However, this approximation is often used by manufacturers of electrical machines to describe the performance of their products.

The second important equation may be determined by looking at the balance of power in the system. If the magnitude of the electrical power which goes into the magnetic field is equal to mechanical power output of the electrical machine:

$$\varepsilon I = F\dot{x} \tag{3.18}$$

than we may derive the expression relating velocity to back EMF:

$$\varepsilon = k_m \dot{x} \tag{3.19}$$

This relation, since it is derived from equation 3.17, is subject to the same caveats. Additionally, the assumption regarding all electrical power going into the magnetic field corresponding to mechanical power is not valid when the electrical machine is subject to large eddy current losses. In practice, sometimes this deficiency is addressed by using different values of k_m for determining force and back EMF. For the linear engine model, a single value of k_m was used in most cases, with separate values applied to the most critical simulations.

Finally, if inductive losses are ignored, then the terminal voltage may be expressed as the sum of back EMF and the coil resistive voltage drop:

$$V_{term} = \varepsilon + RI \tag{3.20}$$

3.1.3 Overall System

Now that a framework for modeling the thermodynamic system and the electrical machine has been established, all that remains is to tie them together. The sum of the force related to pressure and the force of the electrical machine impinge upon the mass of the moving piston assembly. Neglecting friction, this yields:

$$m\ddot{x} = pA - F_{motor} \tag{3.21}$$

This model was implemented in the Matlab Simulink environment (see fig. 3.3.) Approximate parameters (see table 3.2) were determined by comparing simulation results to data from existing HCCI data (see fig. 3.4.) This experiment exhibited large peak pressures when compared to traditional SI operation, but since it was based on part throttle operation, parameters were adjusted to produce somewhat more work in the cycle.

3.1.4 Initial Results

Results of simulation with these parameters are shown in fig. 3.5 and fig. 3.6. The PV diagram is comparable to the experimental data. Actuator forces opposing compression and expansion are significantly larger than actuator forces during intake and exhaust. Peak actuator force occurs as the actuator works to limit the acceleration of the piston while it is being driven downward by combustion forces. Combustion occurs slightly later in the simulation than in the experimental data, but since peak pressure and total work output fulfill expectations, this is not significant to the results. At about .1s, there is a discontinuity in the slope of the graph. This represents

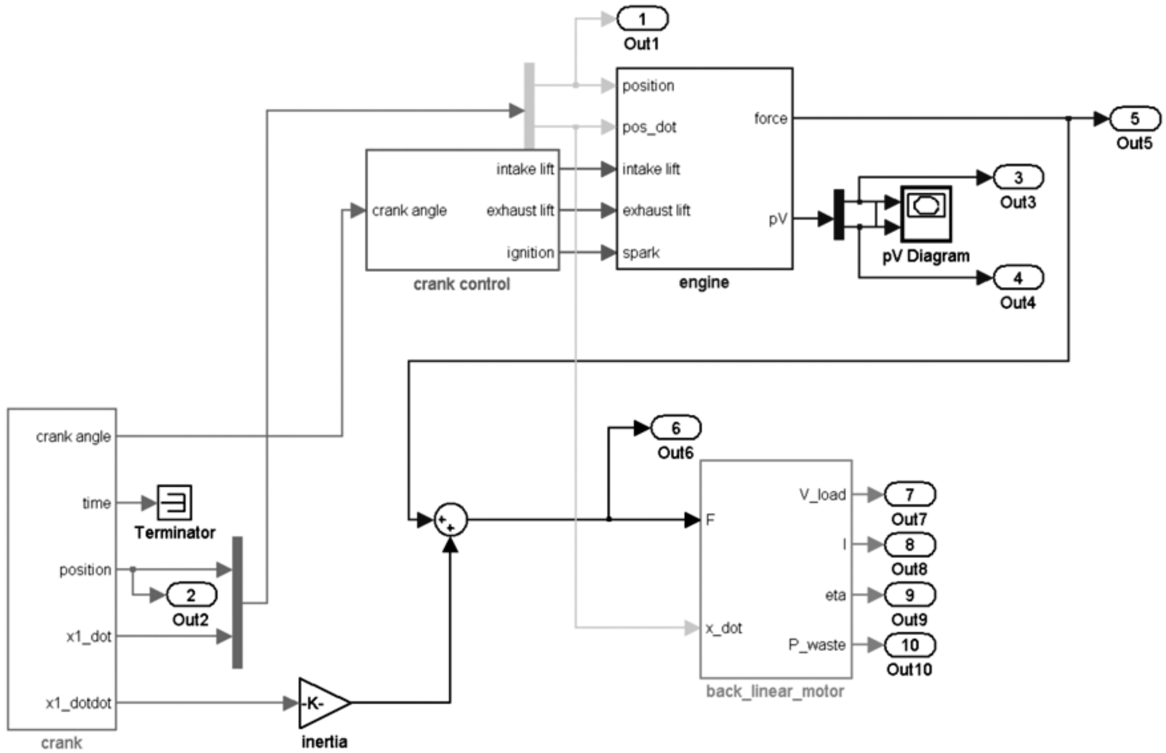

Figure 3.3: Simulink Implementation of Model

Bore	92mm
Stroke	100mm
Compression Ratio	11
Equivalent Speed	900 RPM
Dynamic Mass	16 kg
γ	1.33
R	$287\ \frac{kJ}{kgK}$
$Q_{fuel_{total}}$	750 J
a	5
b	2
t_c	0.0025 sec
c_1	$1 \cdot 10^{-5}\,\frac{kg}{sPa}$

Table 3.2: Engine Parameters

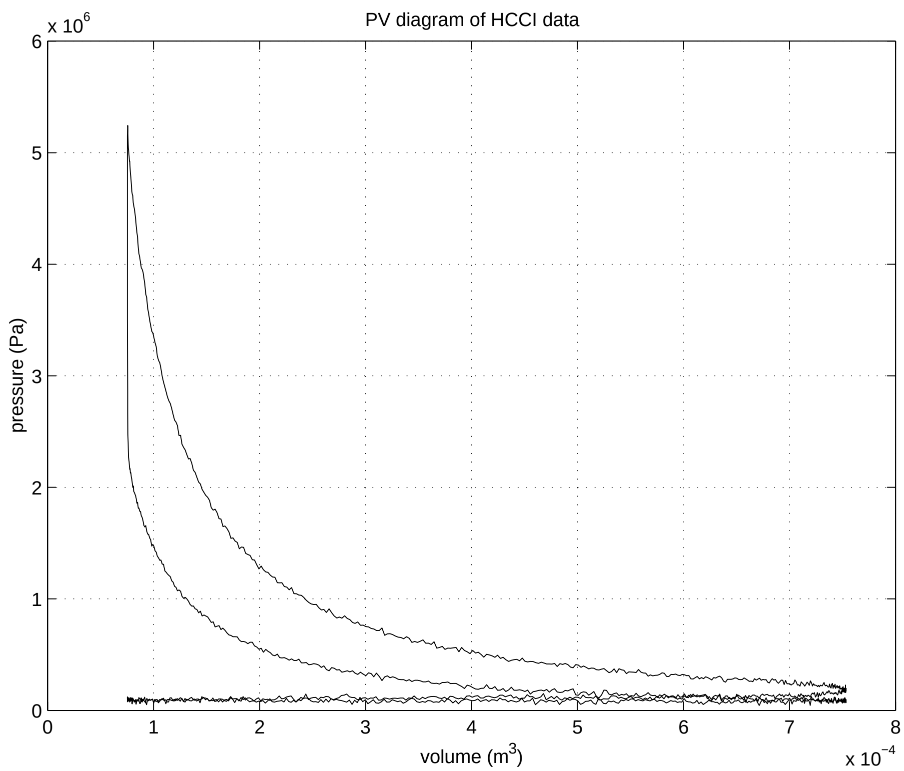

Figure 3.4: Data from HCCI Experiments, courtesy Patrick Caton

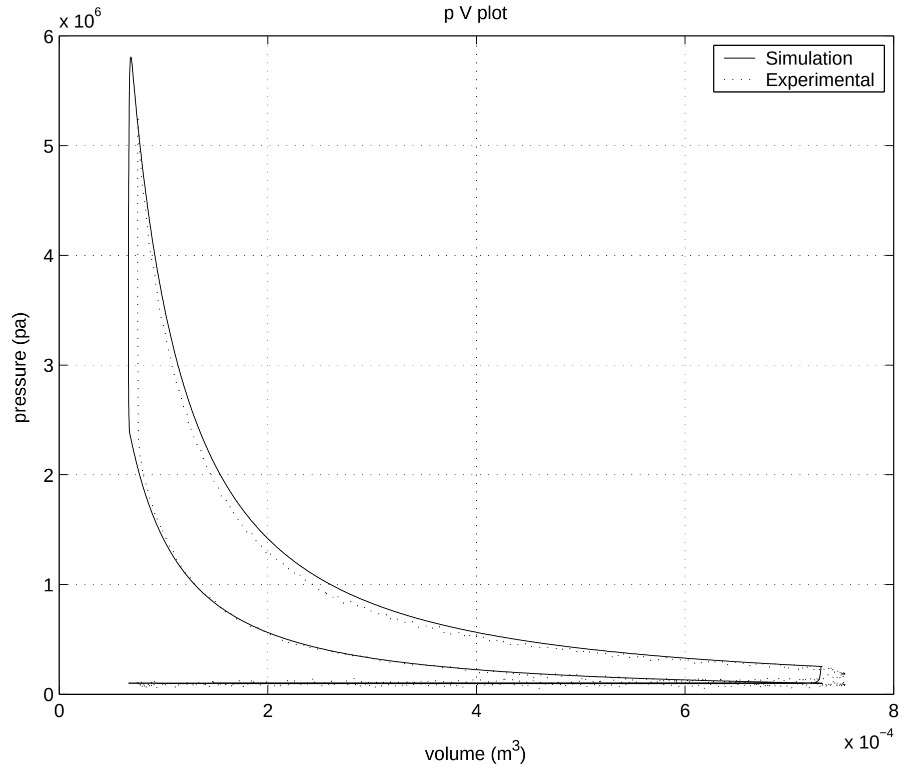

Figure 3.5: PV Diagram

the rapid blow down of gases from the combustion chamber as the exhaust valve is opened.

3.2 Electrical Machine Selection

Based on the results of these simulations, the ideal electrical machine would be capable of supplying a peak force of 30kN and an RMS force of 7.6kN. Piston motion at 16.7Hz with a stroke of 100mm corresponds to a peak velocity of 5.24m/s and a peak acceleration of 56G. Practically, the linear engine had an electrical machine budget of under $20,000, and it was necessary to compromise on some of these parameters. The main implication was that the perfectly sinusoidal motion profile could not be maintained. A key parameter in determining the ability of the electrical machine to

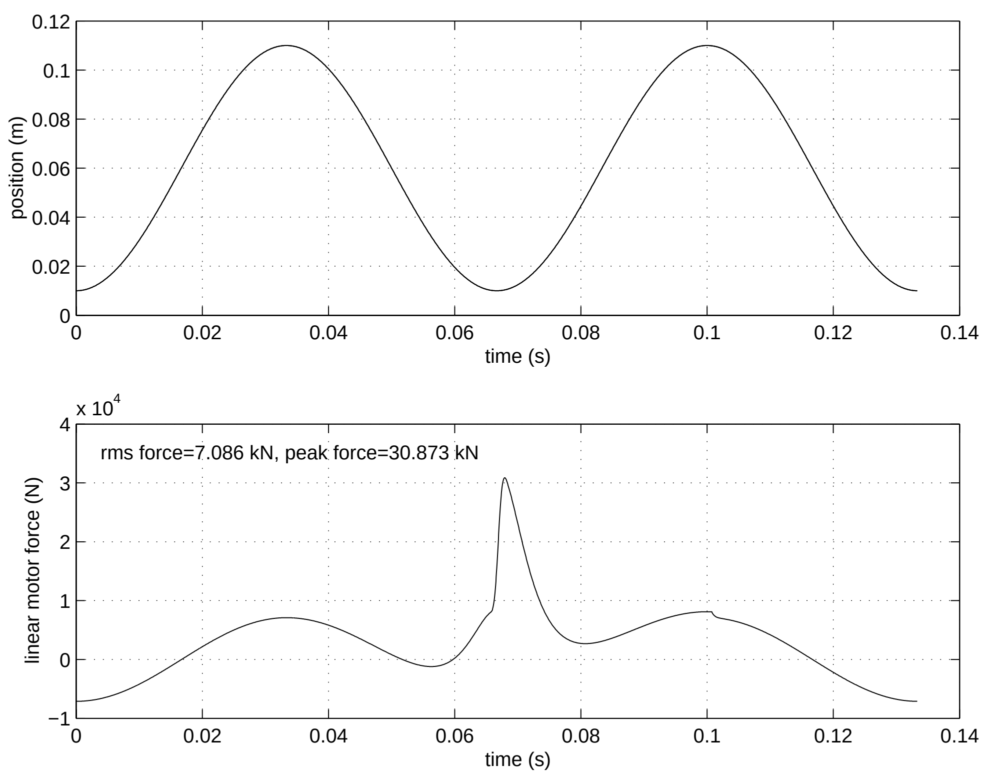

Figure 3.6: Position and Force vs. Time

come close to a sinusoidal trajectory is the theoretical acceleration, which is the ratio of maximum force to rotor mass. A theoretical acceleration of more than 56G was necessary because the total dynamic mass includes not only the rotor, but also the piston and the connecting structure. The necessary acceleration increases with the square of reciprocation rate. However, lower reciprocation rates also mean that the electrical machine must apply more force to slow the piston to a sinusoidal trajectory during the combustion event.

In the requirements definition, it was determined that the electrical machine should be a commercially available system. Fortunately, there are a wide variety of such systems on the market, allowing for the possibility for a good match to the application. In narrowing the field, the main choices were between machines designed as motors vs. generators, brush vs. brushless designs, back iron vs. ironless, AC vs. DC, and linear vs. rotary. These decisions defined a precise type of electrical machine ideal for the application, and the best individual specimen was chosen from this field.

3.2.1 Motor vs. Generator

Most electrical machines may transfer energy in either direction, i.e. from mechanical work to electrical energy, or vice versa. However, machines designed as generators or alternators often use passive power control circuitry, which cannot add mechanical energy to the system. Most electrical machines designed as motors interface with power control systems that can both supply and absorb energy. These systems often burn any excess energy away as heat, but this would only be of importance to a practical power source. Additionally, there is much wider field of commercially available options among motors. Therefore, only motors were worth serious consideration.

3.2.2 Brush vs. Brushless

Some motors achieve commutation via electromechanical brushes. These brushes are usually made of copper, and make electrical contact with a moving series of copper plates. The geometry assures that current passes through the motor coils in the proper direction. But, the brushes may become dirty, and as speed increases, electrical arcing begins to be a problem. Brushless motors control the current through the windings via external switching, typically in the form of a transistor circuit. This avoids the problems of brush commutation, while also allowing for a smoother transition between motor states. While these advantages come at a greater cost, a vendor survey indicated that no available brush motors were feasible for the linear engine.

3.2.3 Back Iron vs. Ironless

Motors often use a back iron on the rotor to improve the magnetic circuit. This iron is quite heavy, so in order to improve the force to mass ratio, some motors employ an ironless design. This is most common in linear motors, and usually results in a higher cost per unit force. However, the force to weight ratio is critical to achieving the high accelerations necessary for engine operation, and the ironless designs have a clear advantage where available.

3.2.4 DC vs. AC

Motors may also be DC or AC, although only rotary motors are available as AC. In practice, for brushless rotary motors, the main distinction is that DC motors employ permanent magnets, while AC motors use windings for both the rotor and the stator. DC motors are usually more efficient, and lighter for a given power rating, but permanent magnets require expensive materials. In general, the need for a good

Manufacturer: Type: Model:	Kollmorgen DC rotary B-808C	WEG AC rotary 404TS Frame
Force (N)	5064	4930
Theoret. Acc.(G)	156	24
Cost	2x $6100	2x $4900
Amps pk-pk	190	230
Mechanical Advantage	12	5

Table 3.3: Comparison Between DC and AC Motors

force to weight ratio seemed to indicate that DC rotary motors had an edge; but, with economic considerations, AC rotary motors might perform better. Thus, a good specimen from each class was chosen, and the two were compared (see table 3.3.) For this application, a rotary motor would require a mechanism to convert rotary motion into linear motion. One can take advantage of this mechanism by selecting a mechanical advantage appropriate to the torque and speed capabilities of the motor. For the comparison, the minimum mechanical advantages which could achieve the peak velocity were chosen, in order to maximize force and the force to equivalent mass ratio. While the two motors performed similarly in output forces, the AC motor was clearly not able to achieve the necessary accelerations and was only 20% less expensive.

3.2.5 Linear vs. Rotary

Finally, motors are available in rotary and in linear configurations. Rotary motors represent a more mature, cheaper technology, and may be used for linear motion via a chain or belt drive, a ball screw, or a rack and pinion. Linear motors, while more expensive, implement linear motion directly without additional complications from a mechanical system.

Manufacturer: Type: Model:	Aerotech DC linear BLMX-502B	Kollmorgen DC rotary B-808C
Force (N)	4744	5064
Theoret. Acc.(G)	109	156
Cost	2x \$5200	2x \$6100
Amps pk-pk	100	190
Mechanical Advantage	N/A	12

Table 3.4: Comparison Between Linear and Rotary Motors

Good specimens from each class are compared in table 3.4. The linear motor has a lower, though acceptable, theoretical acceleration and costs 16% less. However, the cost difference becomes more important when one considers the current necessary to achieve these conditions. The rotary motor requires nearly twice the current, necessitating a significantly more expensive amplifier. Additionally, when one factors in the additional inertia inherent to any practical mechanism to convert rotary motion to linear motion, the rotary motor's advantage in theoretical acceleration disappears. With these considerations, and considering the mechanical simplicity of implementing the linear motor to move a piston linearly, the advantage clearly went to the linear motor.

3.2.6 The Aerotech BLMX-502B

These selections narrowed the field to brushless ironless DC linear motors. Among this field, there are no off the shelf motors with the force capacity the linear engine requires, necessitating that multiple motors be applied in parallel. Surveying several suppliers, such as Aerotech, Kollmorgen, and Baldor, it was apparent that a system of fewer, higher force motors was cheaper and easier to implement than a system of a

Manufacturer	Aerotech	Kollmorgen
Model	BLMX-502B	IL24-100
Number of Motors	2	6
Peak Force (N)	9488	9600
Total Cost	$10,400	$19,530

Table 3.5: Cost Comparison by Quantity of Linear Motors

Figure 3.7: BLMX-502b Coil

larger number of lower force motors (see table 3.5 for a comparison.) Aerotech manufactures ironless linear motors at an exceptionally high force rating (other vendors, such as Kollmorgen, use a back iron design in order to achieve higher force ratings.) Aerotech's highest force system was selected for the linear engine.

The system consisted of two each of the BLMX-502b coil (see fig. 3.7, the MTX720 magnet way (see fig. 3.8), and the BAS100 amplifier (see fig. 3.9.) Key parameters for the system are presented in table 3.6.

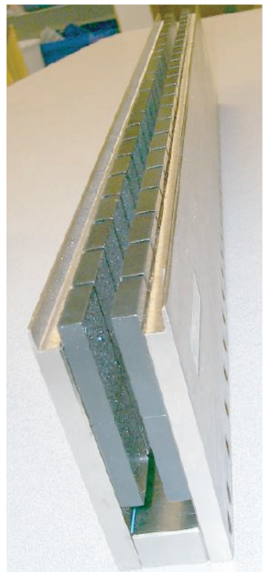

Figure 3.8: MTX-720 Magnet Way

Figure 3.9: BAS-100 Sinusoidal Amplifier

Peak Force	4744.0 N
Max Continuous RMS Force	1186.0 N
k_m for EMF	54.3 $\frac{V_{pk}}{m/s}$
k_m for Force	47.4 N/A_{pk}
Internal Resistance	1.5Ω
Max Terminal Voltage	320 V
Coil Mass	4.45 kg
Coil Length	502 mm
Magnetic Pole Pitch	30.0 mm
Peak Amplifier Current	100 A_{pk}
RMS Amplifier Current	50 A_{pk}
Continuous Amplifier Power	14.4 kW
Amplifier Bandwidth	2 kHz
Total System Cost	$15,903.00

Table 3.6: Key Motor System Parameters

3.2.7 Verification in Simulation

Before an investment was made in the linear motor, additional simulations were conducted based on the specifications of the BLMX-502b in order to confirm that performance is acceptable. While this electrical machine is the best option within the acceptable price range for the linear motor, it was not able to meet the ideal specifications which would allow a perfectly sinusoidal piston motion profile. Therefore, three cases of nonsinusoidal trajectories which were within the capabilities of the motor were studied. The first attempts to track a sinusoid, but deviates slightly as the actuator saturates, the second was based around a wave with varying frequency, and the third demonstrates an implementation of the Atkinson cycle.

Closed Loop Simulation

In order to model actuator saturation, a closed loop controller was formulated for the linear engine. The dynamics of the system may be considered as:

$$\ddot{x} = m^{-1}(pA - F_{mot}) \tag{3.22}$$

With F_{mot} as the control input, this formulation represents the entire thermodynamic system as part of the zero dynamics. Nevertheless, if one has the ability to sense pressure (which is typically the case in research engines) the trivial feedback linearizing controller,

$$F_{mot} = pA - mv \tag{3.23}$$

with v as the new control input, is robust to all disturbances in pressure. Further substituting $v = u + \ddot{x}_d$ to implement feed forward control, with $e = x - x_d$, a trivial LQR controller may be designed for the error system:

$$\ddot{e} = u \tag{3.24}$$

Yielding the overall form of the controller:

$$F_{mot} = pA - m(e \cdot k + \ddot{x}_d) \tag{3.25}$$

With the closed loop, actuator saturation and the resultant deviation in trajectory were simulated (see 3.10.) The deviation is only a small fraction of the total amplitude. Although this behavior is not ideal, clearly the motor can be used for a range of combustion experiments. If it is desirable to more closely approximate crankshaft behavior, a future generation of the linear engine could use four rather than two linear motors.

Variable Rate

This simulation expanded upon the closed loop system described above. But, instead of a regular sinusoid, the system is driven with a frequency modulated sine wave (see

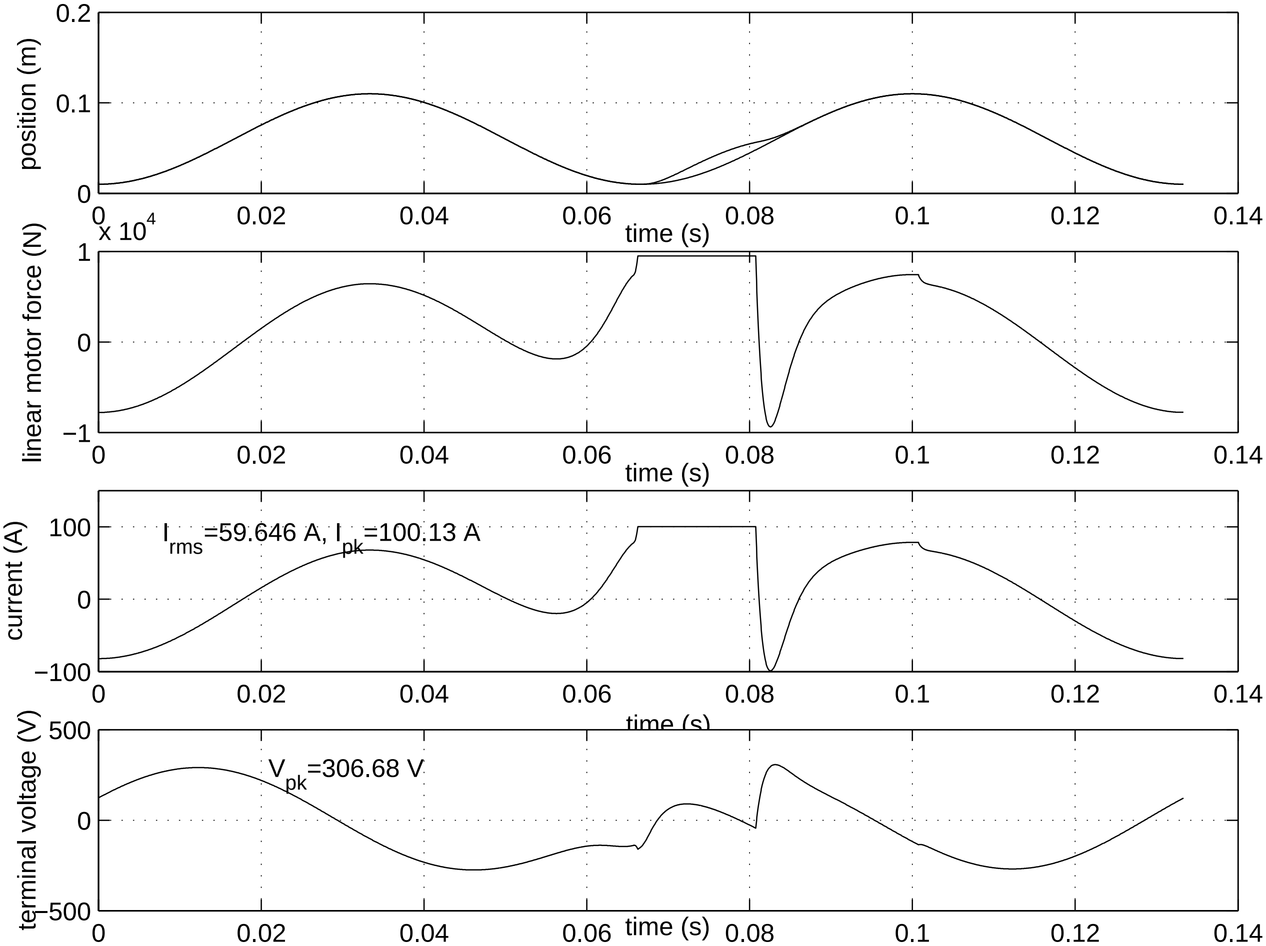

Figure 3.10: Mechanical and Electrical Data for Closed Loop Simulation

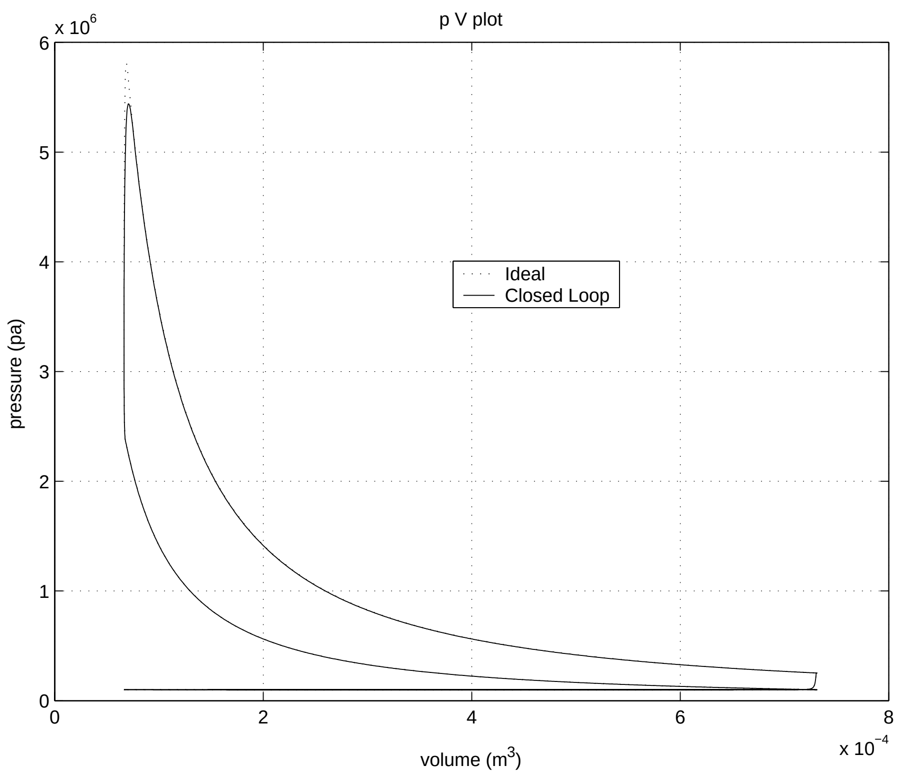

Figure 3.11: PV Diagram for Closed Loop Simulation

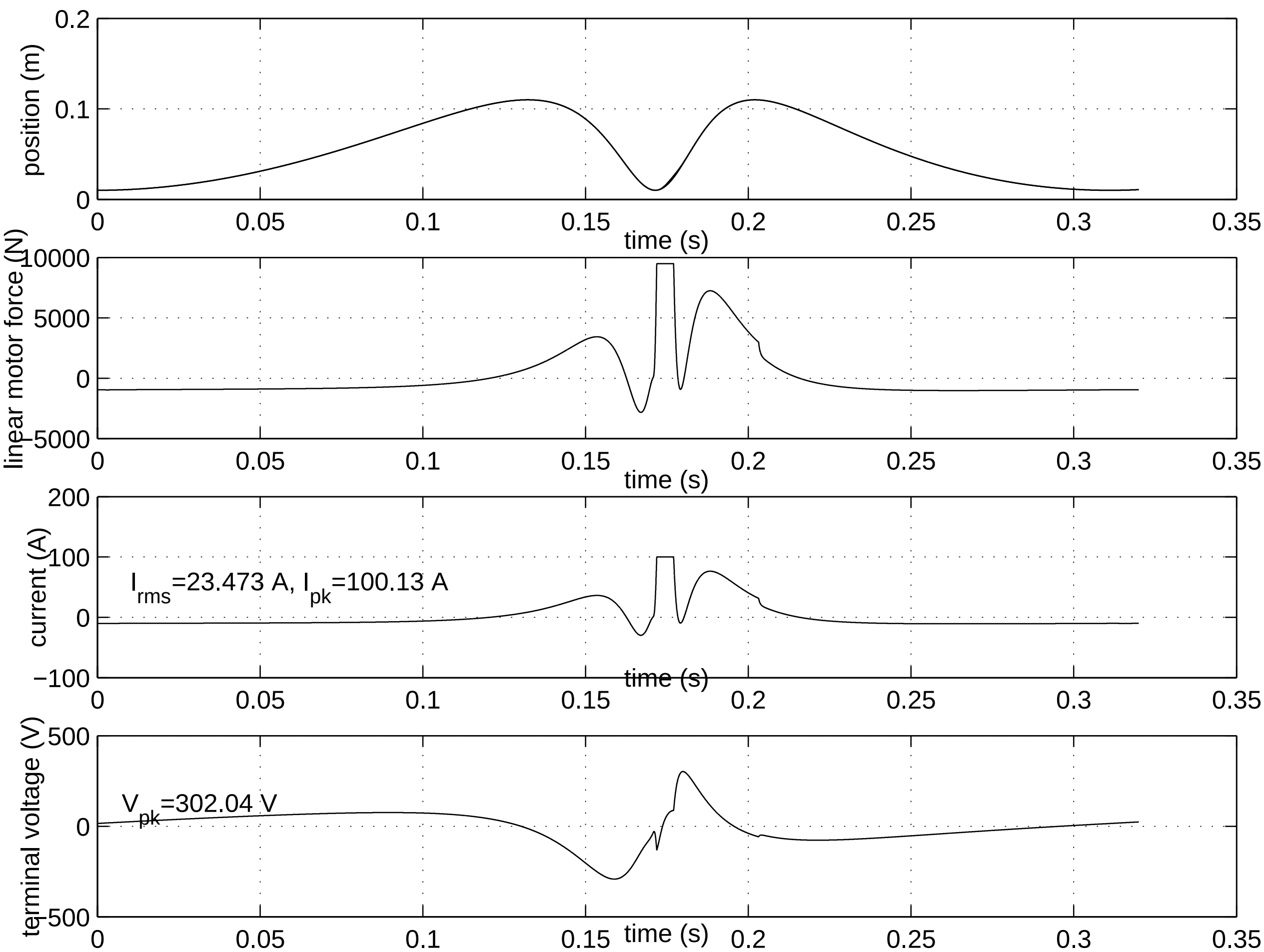

Figure 3.12: Mechanical and Electrical Data for Variable Rate Simulation

fig. 3.12.) The frequency modulation is tuned to increase the rate of acceleration during the expansion stroke in order to reduce the peak force. Then, during intake and exhaust when the piston speed is less critical, the system slows down significantly in order to reduce the RMS force. This motion profile can be sustained by the linear motor indefinitely and results in minor changes to the PV diagram such as a slight decrease in peak pressure (see fig. 3.13.)

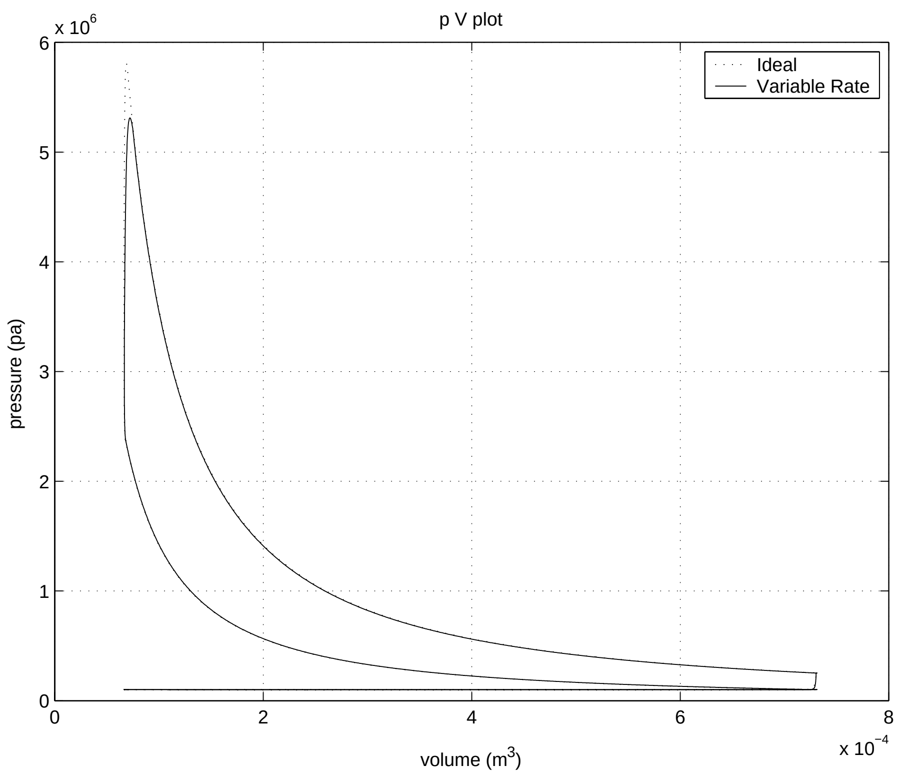

Figure 3.13: PV Diagram for Variable Rate Simulation

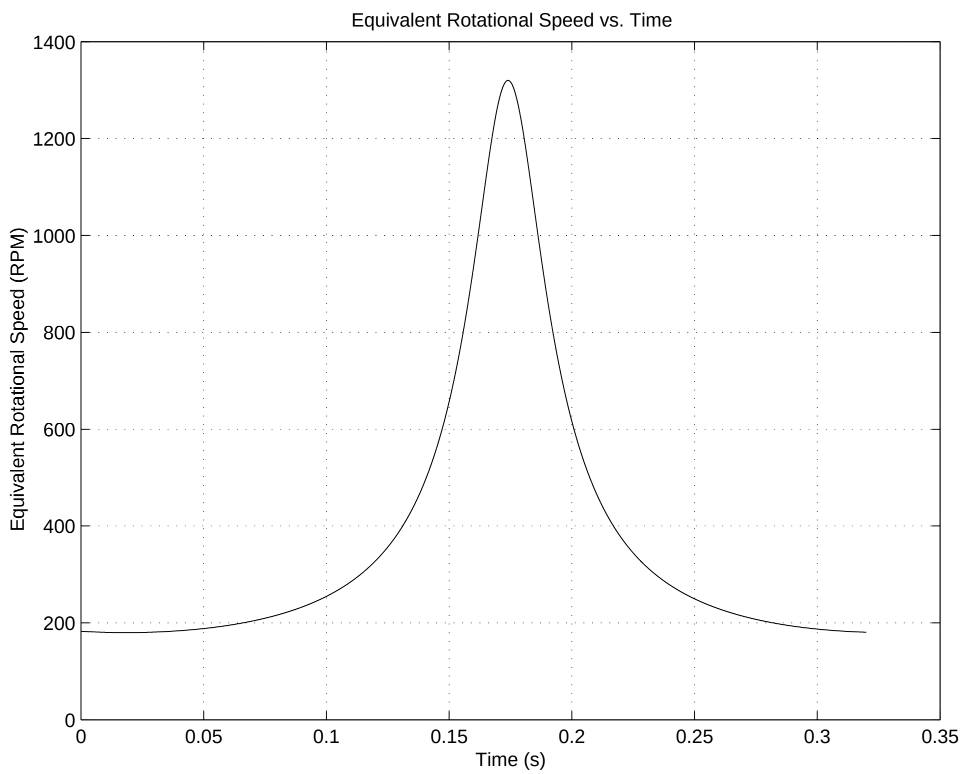

Figure 3.14: Equivalent Crankshaft Speed

Atkinson

As discussed in chapter 1, the ability to implement the Atkinson cycle is an important advantage to employing piston motion profiles unconstrained by a traditional crankshaft. Additional energy is extracted by lengthening the expansion stroke until the cylinder pressure at bottom dead center is near the ambient pressure. A simulation demonstrating the linear engine's ability to implement the Atkinson cycle was carried out by amplitude modulating a sinusoid to create an asymmetric desired trajectory for the piston motion (see fig. 3.15.) Other than the modified command signal, the simulation was carried out as in the first closed loop case described above.

Because of the higher peak velocity due to the larger amplitude in part of the sinusoid, the equivalent rotational speed had to be reduced to 700 RPM in order to avoid exceeding the maximum coil voltage. This lower speed led to slightly greater deviation from the desired trajectory during the combustion event than occurred in the other simulations. For comparison, a simulation was run with a pure sinusoidal motion profile under similar conditions (see fig. 3.16 for the PV diagrams.) The pressure does not quite reach ambient, but extending the expansion stroke further would have yielded diminishing returns in recovered energy while further taxing the velocity and force capabilities of the linear motor. In this simulation, the Atkinson trajectory extracted 6.3% more work then the pure sinusoidal trajectory.

3.3 Linear Motor Prototype

The next step was to prototype the operation of the linear motor. The purpose of the prototype was to learn how to apply the technology, while establishing basic function. Additionally, the prototyping process served to verify key assumptions and parameters about the motor. These goals engendered several requirements of the prototype structure. The magnet way needed to be kept stationary, and the prototype

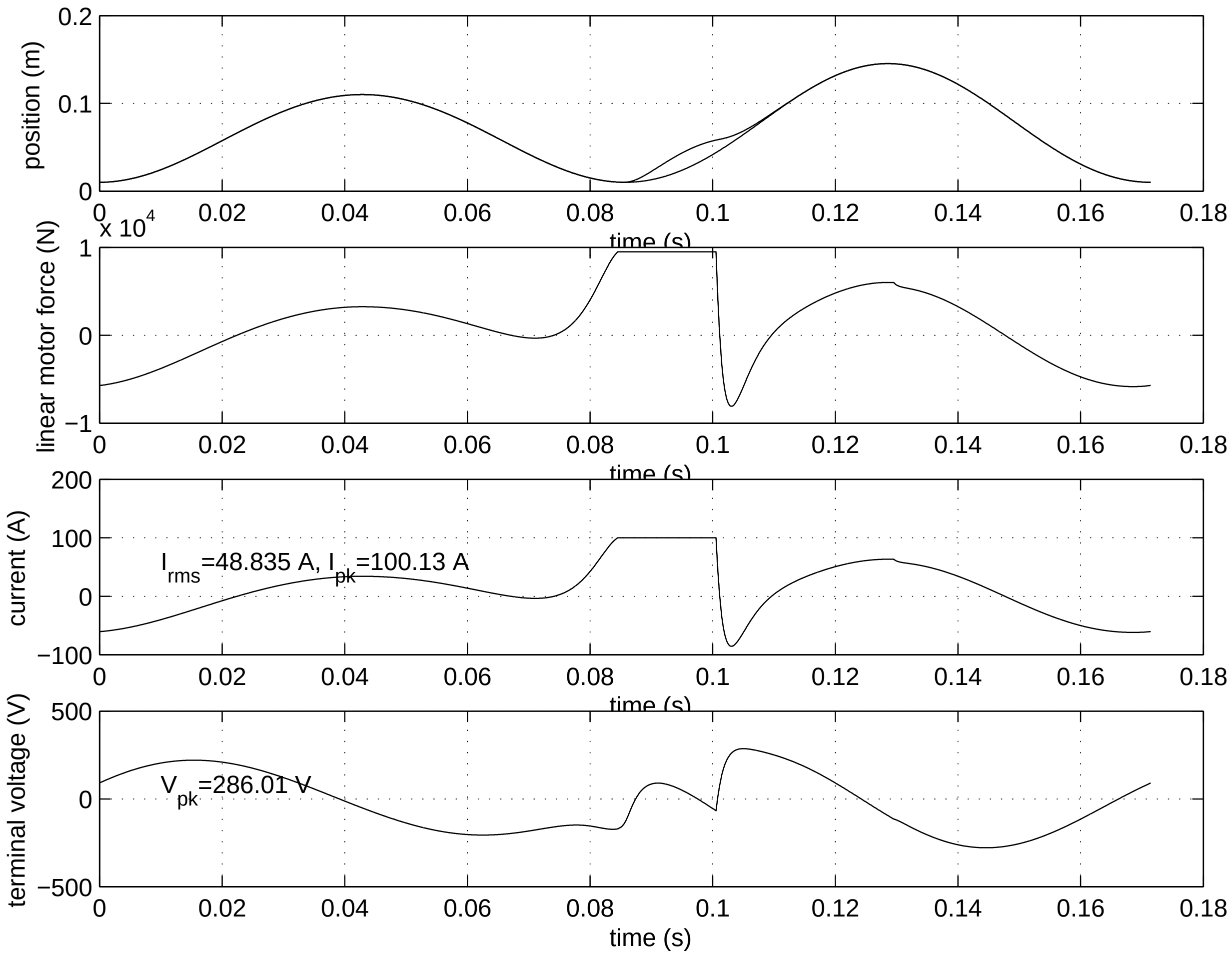

Figure 3.15: Mechanical and Electrical Data for Atkinson Simulation

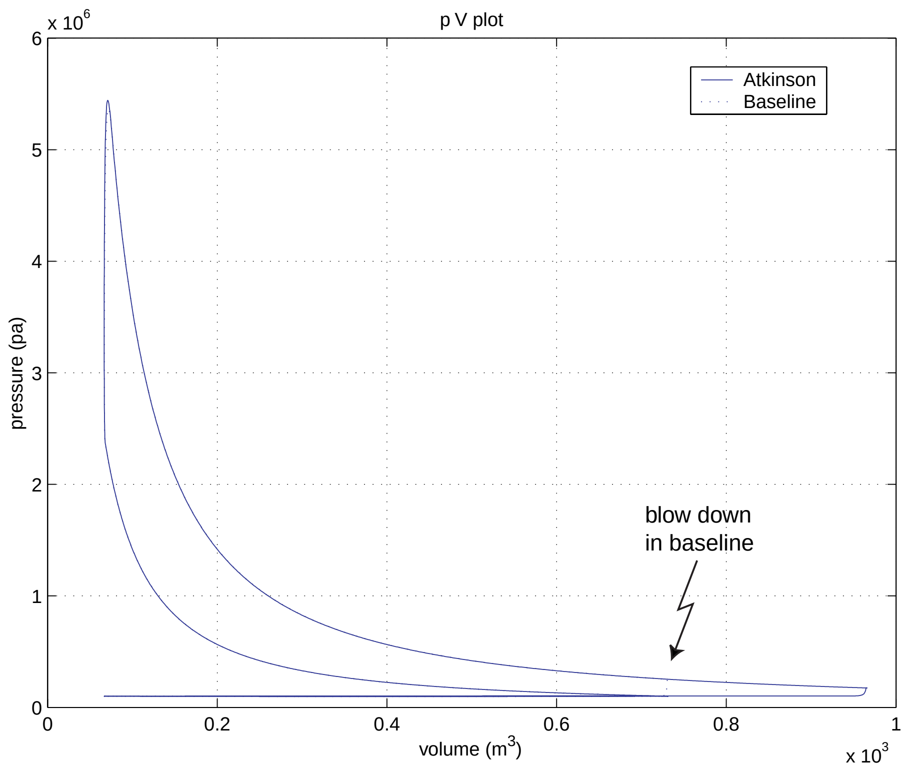

Figure 3.16: PV Diagram for Atkinson Simulation

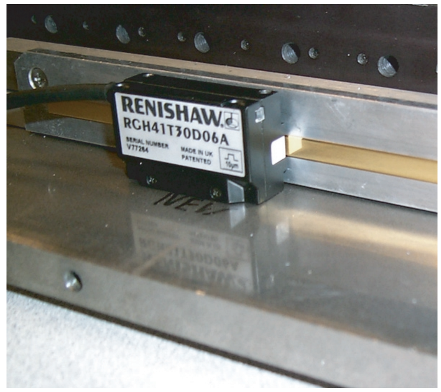

Figure 3.17: Encoder Installed in Prototype

had to constrain the coil to linear motion. The prototype needed to incorporate a linear optical encoder in order to provide position feedback information for sinusoidal commutation.

3.3.1 Components

Early in the process of bearing selection, a free sample of Igus Drylin low profile bearings was obtained. These bearings feature a compact design, have low tolerance requirements, and do not require lubrication. Although it was later determined that these would not be the best bearings for the final design due to their loose tolerances and poor wear characteristics, they were well suited to the needs of the prototype.

The selected linear optical encoder was the Renishaw RGH41T (see fig. 3.17.) Because the encoder was a major investment, it was decided to procure an encoder suitable to the final implementation for the prototype. There were three primary requirements. First, the moving part had to be able to withstand shocks of up to 200G. Second, a resolution of better than 50μm was necessary, in order to report accurate position, and so that an estimator can resolve the velocity in real time. Finally, the encoder had to be reliable at speeds of least 5.24m/s.

The final requirement turned out to be the hardest one to fulfill. The linear

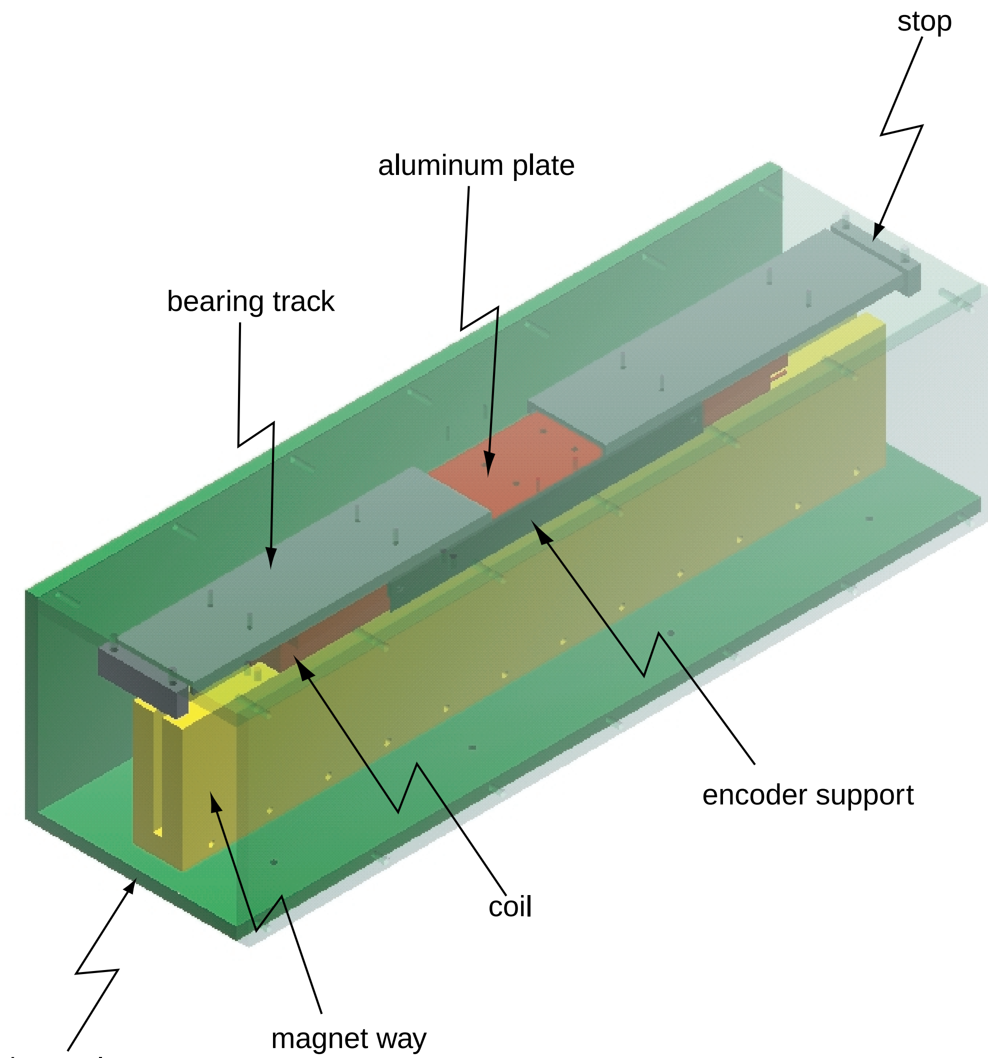

Figure 3.18: CAD Rendering of Prototype

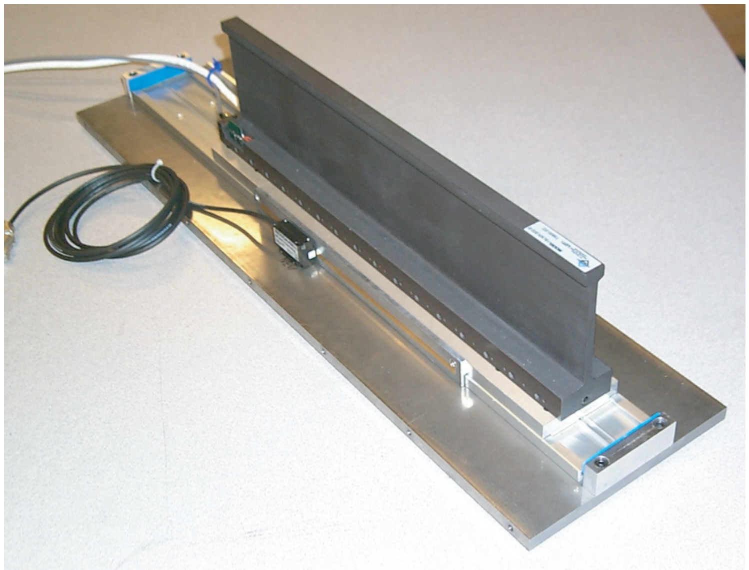

Figure 3.19: Top Portion of Prototype, Inverted

engine's needs for accurate measurement were toward the low end of linear optical encoder technology, but the high bandwidth necessary of the signal conditioning drove prices higher. The Renishaw encoder is capable of handling speeds up to 15m/s, and has a resolution of 10μm. At $598.89 for the complete system, the price was comparable to the nearly equivalent Heidenhain LIDA 177 encoder, but the Renishaw unit had a much shorter lead time.

3.3.2 Mechanical Design

Much of the mechanical design was dictated by a pair of the requirements outlined above: that the magnet way be held stationary and that the coil be constrained to move linearly. The first requirement was fulfilled by bolting the magnet way to a steel base plate, which was in turn bolted to an optics table. The optics table featured heavy steel with a flat surface and precision drilled and tapped holes. The second requirement was fulfilled by bolting additional steel plates to the first, in order to

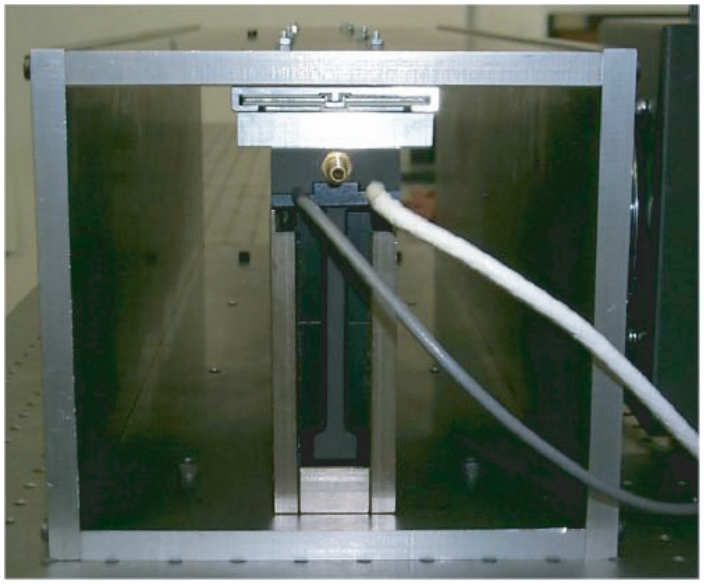

Figure 3.20: End View of Complete Prototype

complete a rectangular prism around the motor. The bearing tracks were then bolted to the top of the box, and the carriages were attached to the coil via an aluminum plate. A CAD model was produced using Solid Edge (see fig. 3.18,) and dimensional drawings were derived from the model (shown in Appendix A.)

Based on these dimensional drawings the parts were machined, primarily via manual mill. Photographs of the completed prototype are shown in figures 3.19, 3.20, and 3.21. In the machining process, efforts were made to maintain critical tolerances within ±0.002in. Although these tolerances were for the most part achieved, the stack of inaccuracies was enough to render the coil unacceptably yawed relative to the magnet way (see fig. 3.22.) This problem was solved by widening the bolt holes through which the magnet way was attached to the base plate, and tightening the bolts while manually constraining the two pieces to the proper configuration. This process indicated some of the difficulties that stacked tolerances may cause for the final implementation. Better manufacturing techniques, or the ability to adjust alignment during set up may be indicated as solutions.

Figure 3.21: Isometric View of Complete Prototype

Additional issues became apparent upon assembly. Each bearing carriage rode upon a separate track, and both carriages needed to be inserted into the tracks at the same time. Aligning the carriages for insertion into the secured tracks was nearly impossible, and one of the tracks had to be left unfastened until the carriages were both completely inserted. Once again, this raises a major issue which must be addressed for the final implementation. Depending on the predicted cycle of assembly and disassembly, it may be necessary to include better means to align the components for easy assembly.

After the initial assembly, two additions were deemed necessary for the design. The first was a pair of mechanical stops, to keep the coil from leaving the magnet way. These consisted of aluminum blocks bolted to the top plate, with a small sheet of energy absorbent polymer on each of them. The second was a stress relief for the power and data cables exiting the coil. This consisted of a single piece of aluminum which was screwed into the coil mounting surface, to which the cable was secured. This was necessary in order minimize fatigue damage to the cables, which cannot be

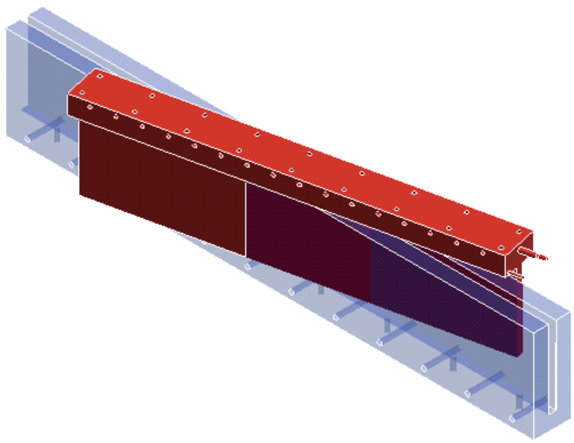

Figure 3.22: Exaggerated Misalignment between Coil and Magnet Way

replaced without disassembling the coil. These additions completed the mechanical design of the prototype.

3.3.3 Integrating the Electronic System

Now that the mechanical system was in place, it was necessary to integrate the electronic system. This process consisted primarily of connecting the power, the coil, and the optical encoder to the BAS-100 amplifier (see fig. 3.23.) The input power and the power level connections to the coil were attached to the screw terminals on the amplifier. The data level connections, from the encoder and the hall effect sensors on the coil, were distributed to conductors on the D-SUB connectors of the BAS-100 via a breakout box.

Once the electrical connections were secure, parameters were programmed into the amplifier through a Windows based control program. These parameters indicated such information as the resolution of the encoder, and whether the amplifier

Figure 3.23: Electronic Interface

should operate in current or velocity control mode. Once these were set, an oscillating signal from a function generator was connected to the control input in order to test the system. After locating some bad connections, the motor moved smoothly and vigorously in response to frequencies ranging from 0.5 Hz to 30 Hz (1000 RPM corresponds to reciprocating piston motion at 16.7 Hz.)

3.4 Experimental Determination of Motor Constant

The motor constant, as described in section 3.1.2, relates the current in the coil to the force produced by the motor. Because the amplifier accepts a voltage input which is proportional to current output, it is necessary to know the motor constant in order to control motor force. This is especially true if the motor force is controlled open loop, but even if the motor/amplifier system is incorporated into a servo loop controlling

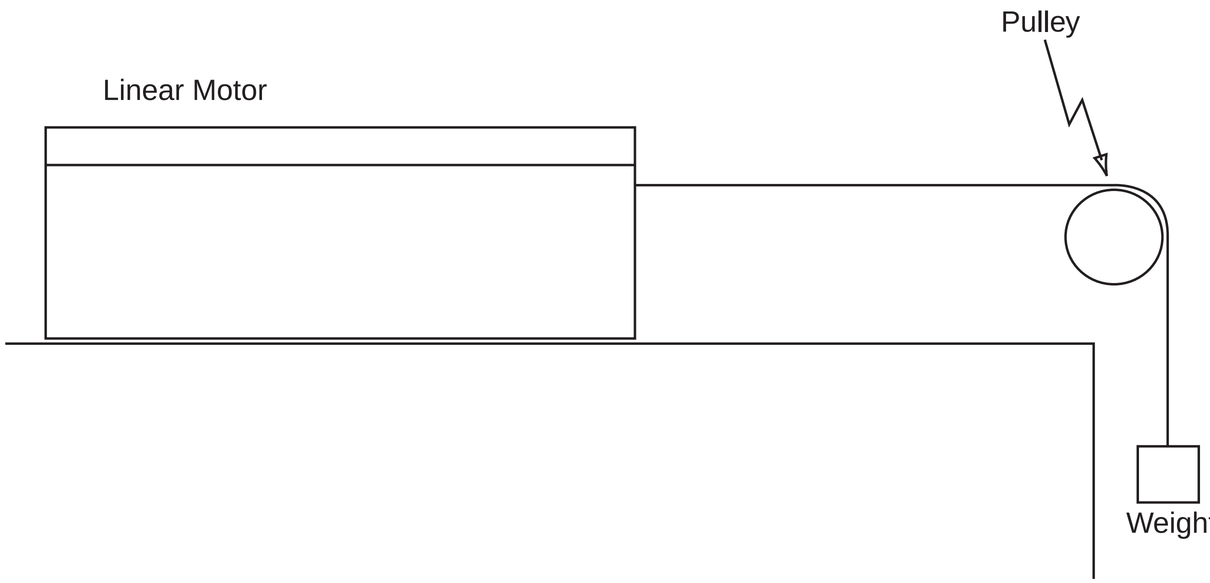

Figure 3.24: Pulley Arrangement

force or position, it is necessary to have some knowledge of the plant in order to design and verify the controller.

Aerotech specifies a value for the motor constant, but they list an uncertainty of +/- 10% on all values, to account for manufacturing variations and fluctuations related to usage patterns, such as those due to temperature. Additionally, the motor constant is an approximate description of the relationship between current and force, and may have limited accuracy in some electromechanical systems. Therefore, it was important to experimentally verify the motor constant. Then, if the measured value was close to Aerotech's, it would also be further evidence that the motor as implemented in the prototype was functioning properly.

An experimental procedure was developed to measure the motor constant, by applying a known constant force via a weight and measuring the current in the coil necessary to oppose this force. All measurements were taken with the coil stationary, so that time averaged readings could be taken. Measured values for the motor constant were significantly lower than the listed value for low forces, but at higher forces

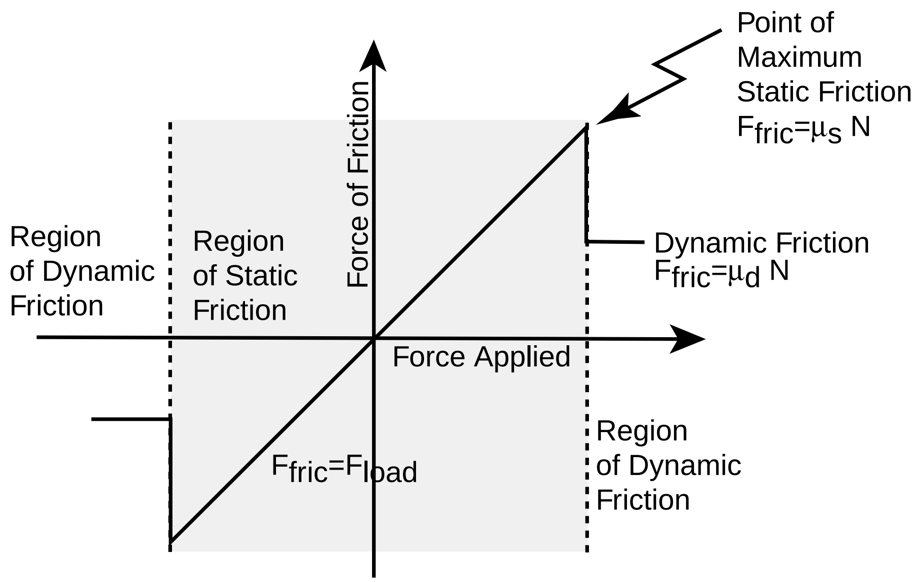

Figure 3.25: Static Friction

the values were much closer.

3.4.1 Applying a Known Constant Force

An arrangement with a pulley and weight was used to apply a known constant force to the coil (see fig. 3.24.) The force applied by a weight is consistent, and for the calibrated weights used for the test, accurately known. However, there is also friction in the system. When the system is moving, no doubt dynamic friction is significant, but for the stationary measurements desirable for these experiments, static friction was the primary concern. Static friction opposes forces which tend to move an object at rest. It will exactly oppose these forces until they exceed the maximum static friction (see fig. 3.25.) At this point, the object will begin to move, and likely accelerate, because the dynamic friction is typically less than the maximum static friction.

Therefore, in order to apply an accurate force, it was necessary to account for the static friction. This was accomplished by identifying the limits of static friction in both directions of movement. First, the current was adjusted so that the motor force was somewhere in the range where the coil remained still. Then, the force was progressively reduced, until the coil began to move in the direction which lowered the weight. This corresponds to the point at which the force due to the weight exceeded the force applied by the coil plus the maximum force of static friction, or,

$$f_{motor} = f_{weight} - f_{friction} \tag{3.26}$$

Second, the motor force was progressively increased until the coil began to to move in the direction which lifted the weight. This corresponds to the force in the motor being equal to the force due to the weight plus the maximum force of static friction,

$$f_{motor} = f_{weight} + f_{friction} \tag{3.27}$$

This procedure was repeated five times in each direction. The input voltage to amplifier was noted each time, and an average was found for each direction. The midpoint of these two voltages corresponds to the current which yields a motor force equal to the weight:

$$f_{motor} = \frac{(f_{weight} + f_{friction}) + (f_{weight} - f_{fric})}{2} \tag{3.28}$$

3.4.2 Measuring the Current

Once the motor is opposing a known force, the current must be measured in order to determine the motor constant. The BLMX-502B is a 3-phase brushless DC motor, and therefore contains three independent circuits. The amplifier, based on position information from the hall effect sensors and the optical encoder, commutates the current input to each of these circuits. At a constant voltage input to the amplifier, the current in each of the three circuits should trace out a sinusoid as the coil is moved through one complete electrical cycle (corresponding to 60 mm displacement.) Current related data is reported by Aerotech in terms of RMS current in a single circuit. Therefore, in order to measure the current, the coil was moved through two complete electrical cycles (120mm), and the current in one coil measured at each point. A pair of measuring surfaces was identified to determine the position of the coil via digital callipers, and a convenient point was designated as the origin of measurement.

A Hall Effect based current sensor was installed on the lead to Phase A of the coil. This sensor outputs a current proportional to the current it is sensing. This output was conditioned via a current-to-voltage amplifier and a 2-pole Sallen-Key lowpass, designed for a cutoff frequency of about 450 Hz. The voltage from this circuit was read on an HP5460B oscilloscope via a 10X probe. Since all measurements were static, the "voltage average" function of the scope was exploited to directly read numerical voltages. The current sensor was calibrated by installing the sensor on a wire placed across the terminals of the power supply. Currents were set from the power supply, and the resulting voltages were read from the scope. The results were generally well behaved and linear (see fig. 3.26). A least squares fit to a line was performed on this data.

For each experiment, the coil was placed at the origin and a reading of the current sensor was made. This procedure was repeated at 3mm increments as the coil was moved through 120mm.

3.4.3 50 lb Weight Trial

The above procedure was applied using a 50 lb weight. This resulted in an input voltage of 822 mV, or about 8.2% of full scale. The voltage readings were converted to currents based on the results of the calibration (see fig. 3.27.) Maximum static friction was measured as 8lb.

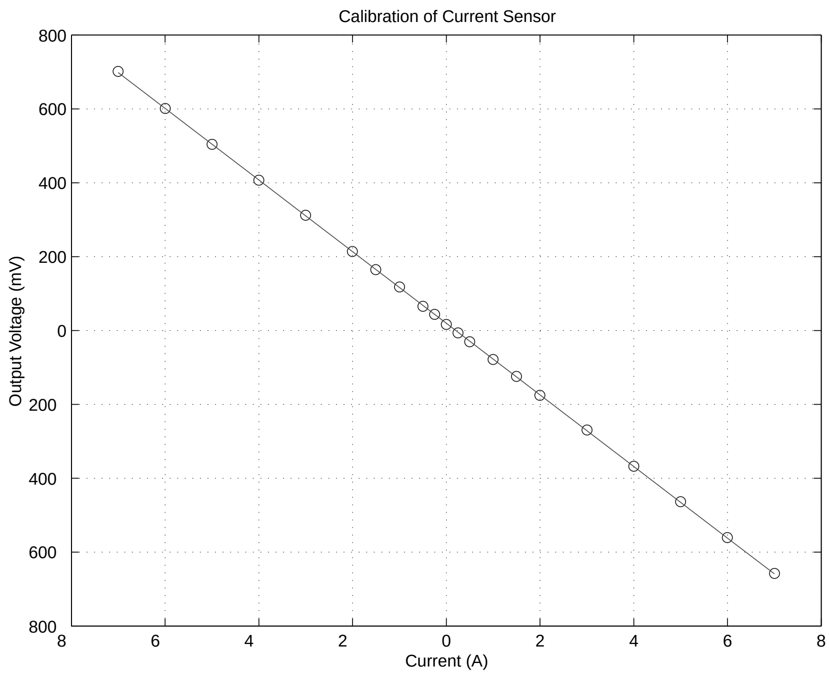

Figure 3.26: Current Calibration

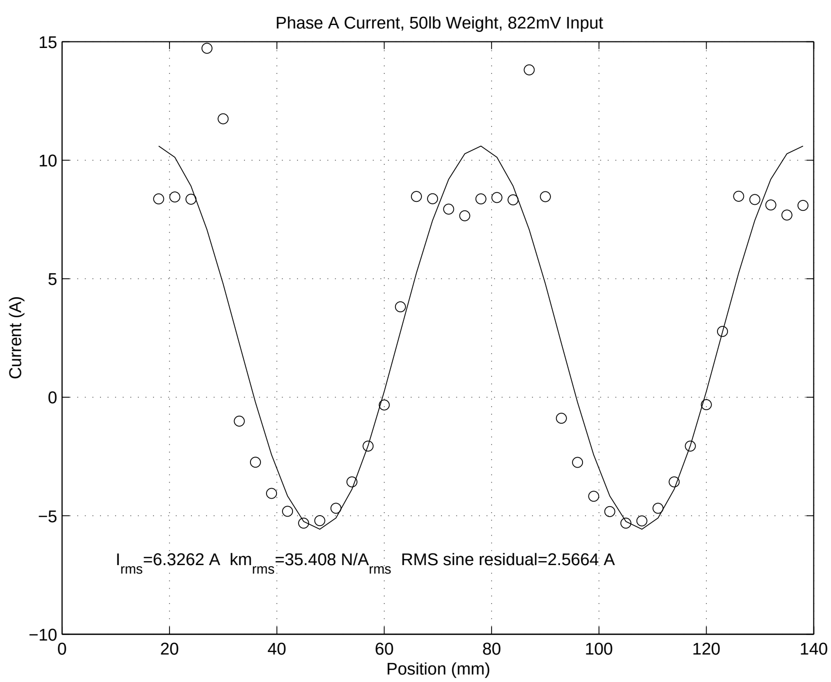

Figure 3.27: Current vs. Position, 50 lbs.

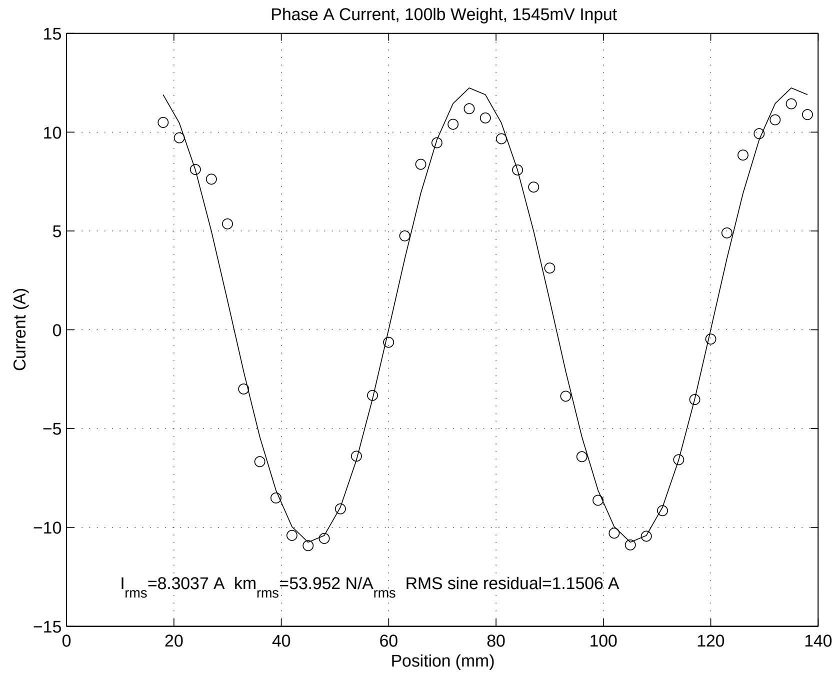

Figure 3.28: Current vs. Position, 100 lbs.

The results were somewhat troublesome for two reasons. Firstly, there is a significant deviation from a sinusoidal trajectory. The best fit offset sinusoid (via least squares,) shown imposed upon the data in fig. 3.27, leaves residuals with an RMS value of $2.57A$, or 41% of the total RMS amplitude. Secondly, the measured k_m was $35.4N/A_{rms}$, whereas Aerotech lists a value of $67.0N/A_{rms}$.

The waveform seems to repeat itself fairly precisely, suggesting that measurement noise was not the dominant factor. Additionally, measurements were taken of the other phases by manually moving the coil at a constant velocity and examining the traces on an oscilloscope. The wave shapes were similar for all three phases.

The input to the amplifier remained constant, and conditions did not approach saturation. Therefore, if there was no measurement error, and the hall effect and encoder signals were functioning properly, the amplifier must have some problem maintaining a sinusoidal current profile.

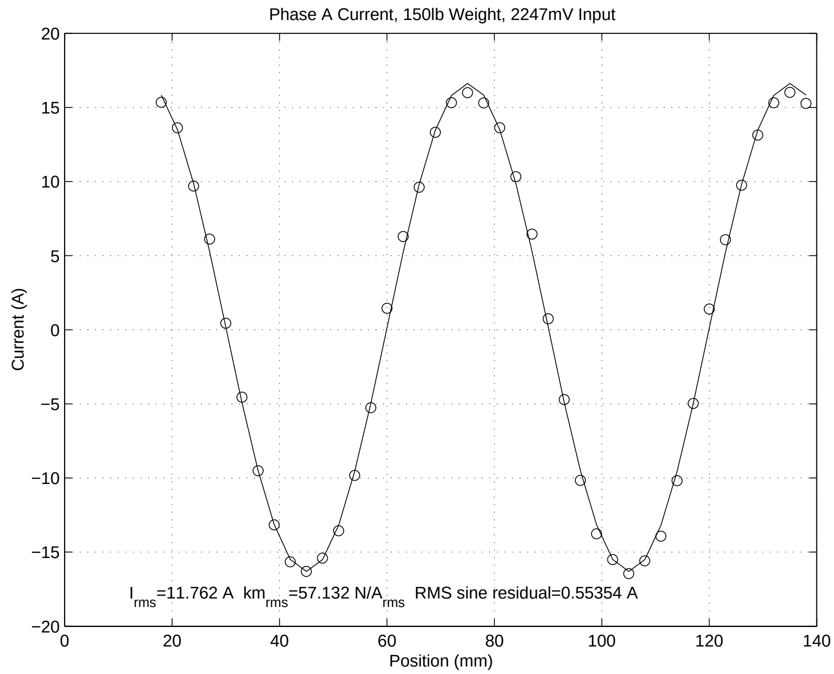

Figure 3.29: Current vs. Position, 150 lbs.

3.4.4 100 lb and 150 lb Trials

50 lb is only about 5% of the peak rating for the coil and the amplifier. On the premise that these problematic effects may be related to nonlinearities which would be less apparent at higher currents and larger forces, further trials were conducted. Measurements were taken using the above procedure at 100lbs and at 150lbs (see figs 3.28, 3.29.) Static friction was measured as 16lb for the 100lb experiment, and 25lb for the 150lb experiment.

It is readily apparent that the current profile is a much smoother sinusoid at the higher force levels. The improvement is clearer when one examines the RMS value of the residuals for each of the three trials (see fig. 3.30.) This result is clearer still when compared as a proportion of the RMS current of the wave; whereas, at 50lbs, the magnitude of the error is 40.5% of the magnitude of the wave, and at 150lbs, the error is only 4.7% of the total.

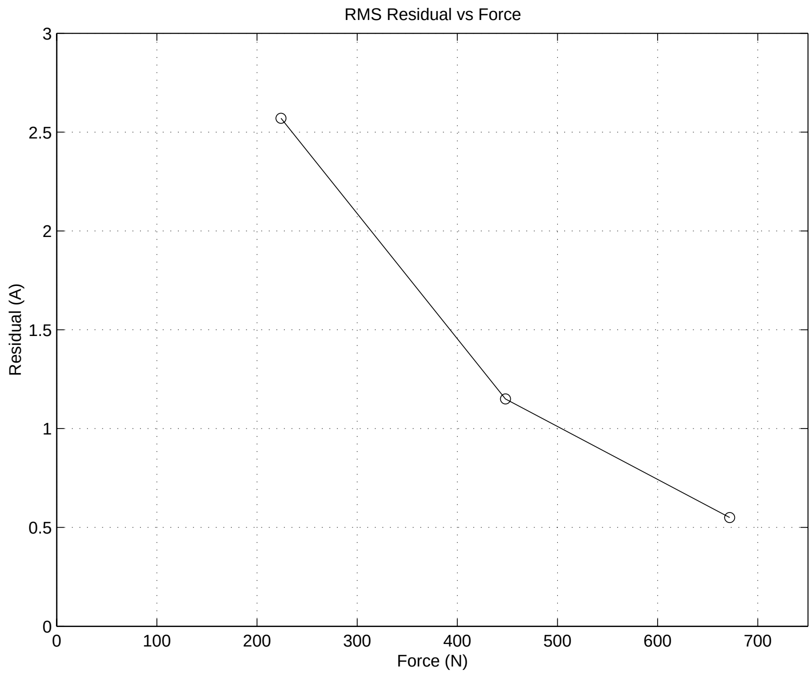

Figure 3.30: RMS Value of Residuals for Different Loads

Also, the measured motor constant is higher at the higher loads, bringing it closer to the Aerotech specification (see fig. 3.31.) The measured k_m at 150lbs, $57.1N/A_{rms}$, is 14.8% short of the specified value of $67.0N/A_{rms}$ (Aerotech lists a tolerance of +/-10% on it's specifications.)

3.4.5 Discussion

These results suggest that the motor/amplifier behave approximately as expected when the current is above a certain threshold (perhaps 10-15% of peak current.) However, at lower current levels, the commutation appears to be nonsinusoidal, and the motor constant is significantly lower. The exact design of the BAS100 amplifier is proprietary, but based on information in the documentation and standard practice, it is probably functionally similar to the schematic in fig. 3.32. In order for the output to deviate significantly from the sinusoid, it is likely that the feedback loop in this circuit

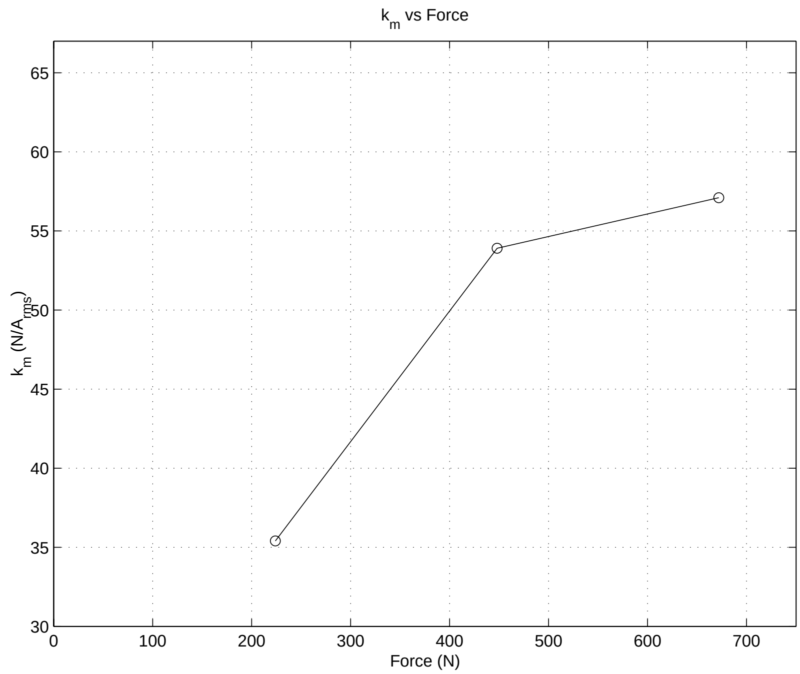

Figure 3.31: Motor Constant at Different Loads

is poorly designed for low current operation. However, at higher RMS currents the low current segments of the sinusoid are well formed, so it is difficult to fully explain this behavior. It is reasonable to conjecture that the low motor constant is related to nonlinearities in the development of the magnetic field.

In any case, given the existence of this nonideal behavior, there are implications for the implentation of a control system. It may be that the low force scenario is not encountered during critical segments of the linear engine's usage cycle, and that the resulting deviations may thus be tolerated. If this does not turn out to be the case, then steps must be taken to either identify the relationship between current and force more accurately and compensate for it in an open loop system, or to close the loop to create a servo with an adequately robust control algorithm.

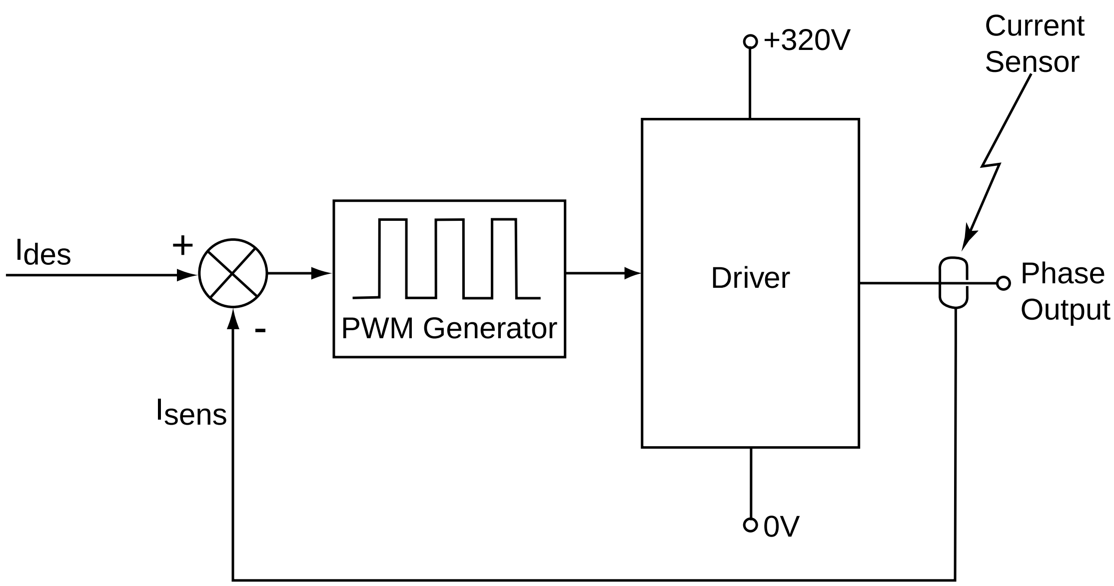

Figure 3.32: Schematic of Amplifier Output Stage for a Single Phase

Chapter 4

Design Specifications

After the design was developed by simulating the linear engine, and selecting and prototyping the linear motor, the remaining step in establishling feasibility was to sketch out the design specifications for the linear engine. First, several additional necessary components were identified and selected. A set of ceramic pillow block bearings from LM76 was chosen to constrain the dynamic assembly to linear motion. In order to absorb the energy of motion from the system in the event of an emergency stop, aluminum honeycomb material was selected for the top of the stroke and a hydraulic shock absorber from EfDyn was selected for the bottom of the stroke. Dynamic cabling from Olflex was specified. Finally, an overall mechanical design for the linear engine is suggested, taking into account geometrical constraints and force requirements.

4.1 Linear Bearings

The purpose of the linear bearings is to constrain the moving portion of the linear engine to translation along a single axis without rotation. In order to do this, they must provide as little hindrance as possible to motion along the primary axis, while allowing little compliance in other directions. This means providing hard, low friction surfaces which will wear minimally and evenly.

The linear engine imposed three important quantititative requirements on prospective linear bearings: that they be capable of withstanding velocities of up to 5.24m/s, shocks of at least 56G, and off-axis forces corresponding to the peak axial load of nearly 10kN. The final requirement is not difficult; the actual side forces likely to be encountered are not more than 10% of the total, and these are not loads of unusual magnitude for bearing applications. The velocity and the shock requirements, however, necessitated special attention.

The most obvious bearing technology is ball bearings. Ball bearings offer excellent wear characteristics, high dimensional accuracy, and the lowest friction. However, most ball bearings investigated could not withstand a velocity of 5.24m/s, and no ball bearings which could sustain shocks of above 50G were identified. These extreme conditions lead to surface and fatigue failures of the intricate mechanical components in ball bearings.

Therefore, we explored the space of bearing technologies with few moving parts. One category of bearings depends on a sacrificial material. In these bearings, a soft material moves against a harder material. The softer element gradually wears down, and must be periodically replaced. The Igus bearings were one example of this technology. These bearings feature a flat carriage with Drylin nylon inserts which interface with an aluminum track. This solution was compact and inexpensive, and constrained the bearings in rotation. However, the tolerances were not good, and after a series of test assemblies for the linear motor prototype, a significant degradation in tolerance was noted.

Some of these tolerance issues might be attributed to the design of the Igus low profile system. The critical dimensions are determined by the interface between a molded plastic part and an extruded aluminum piece. The traditional ball bearing

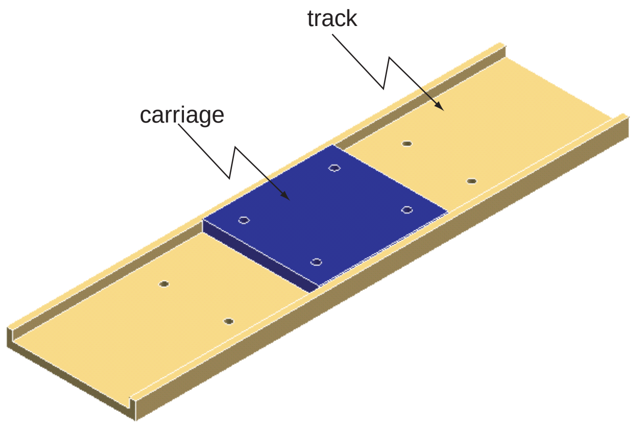

Figure 4.1: Schematic CAD Model of Igus Bearing

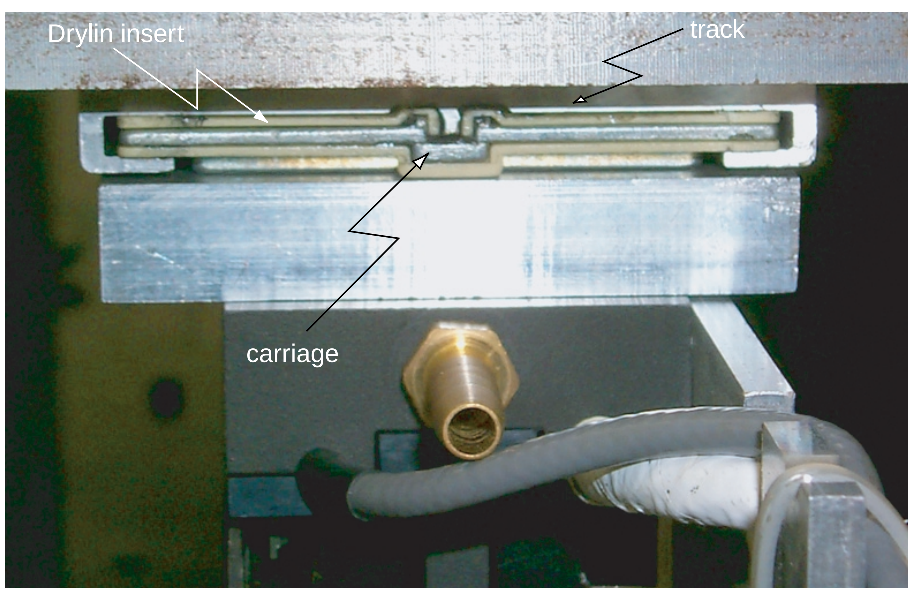

Figure 4.2: Photograph of Igus bearing in Prototype

style configuration, in which a circular bearing moves along a ground shaft, is far more likely to yield good tolerances.

There are bearings based on sacrificial materials which use this design. Igus makes Drylin bearings which use this design, and there are a variety of brass bushings on the market. These systems involve a few hundred dollars investment in shafting and supports, and often in pillow blocks, with the bearing itself accounting for perhaps 5% of the cost of the total system.

Based on these economics, it made sense to consider investing in a more exotic material for the bearing. Pursuing this logic, we discovered the ceramic bearings manufactured by LM-Tarbell. Like the sacrificial technologies, these bearings featured a single piece surface which moves along a steel shaft. However, because these bearings use a very hard, smooth, ceramic material, both surfaces experience very little wear. At the micron level, asperities are worn in slightly at the beginning of service. After this period, for the effectively infinite life time of the bearing system, the two surfaces interact only via a thin film of oil. Grease must be applied to the shaft occasionally, but otherwise, the system requires little maintenance. Tolerances are primarily dependent on the quality of the shafting, and are typically better than 40μm. Load capacities are high, and friction is lower than Drylin or brass (μ is typically better than 0.050 N/N, with proper lubrication.)

Based on maximum off axis forces of 1 kN on each bearing, and trying to minimize compliance in the shafting, a shaft diameter of 20mm was selected. Open bearings were used in order to support the shaft along its entire length. In order to avoid binding, and constrain rotation, a total of four bearings on two shafts were used. Model number MXPB20 pillow block assemblies were selected and procured (see fig. 4.3 and 4.4.)

LM-Tarbell was not able to supply shafting. In order to assure a good bearing surface, the shafting needed to be made of high quality ground steel. Also, it needed

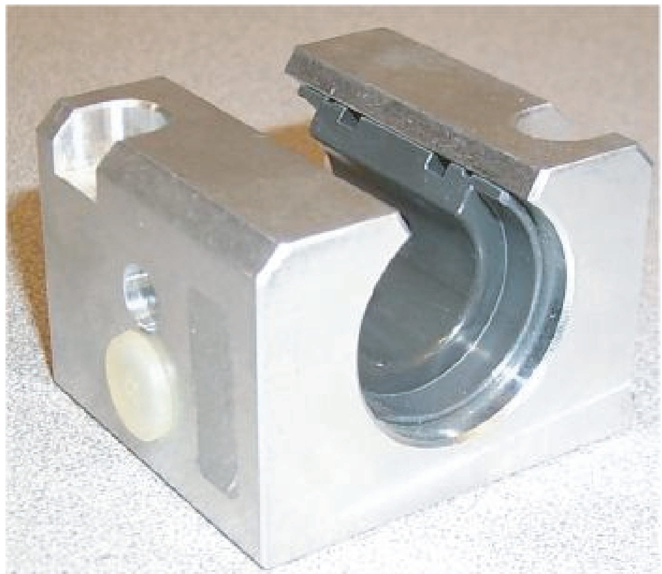

Figure 4.3: Ceramic Bearing and Pillow Block

to have holes along its length and a support in order to fasten it to a flat surface. The most economical option that fit our requirements was the LSRA M20 shafting system from Thomson (see fig 4.5.)

4.2 Energy Absorption

The estimated mass tally for the dynamic portion of the linear engine was 16kg, moving at more than 5m/s with an actuator force of 10kN, and even higher forces due to combustion. If a failure were to occur such that the system could not be controlled under these extreme conditions, great damage could be done to the expensive apparatus, and more importantly to any person who happened to be nearby. Therefore, it was extremely important to build in effective means of stopping the dynamic element.

Because of the bearing system, the moving assembly can only move along one axis. Therefore, in order to handle a failure, stops needed to be applied to both extremes of the stroke. There were distinct requirements for these two stops since

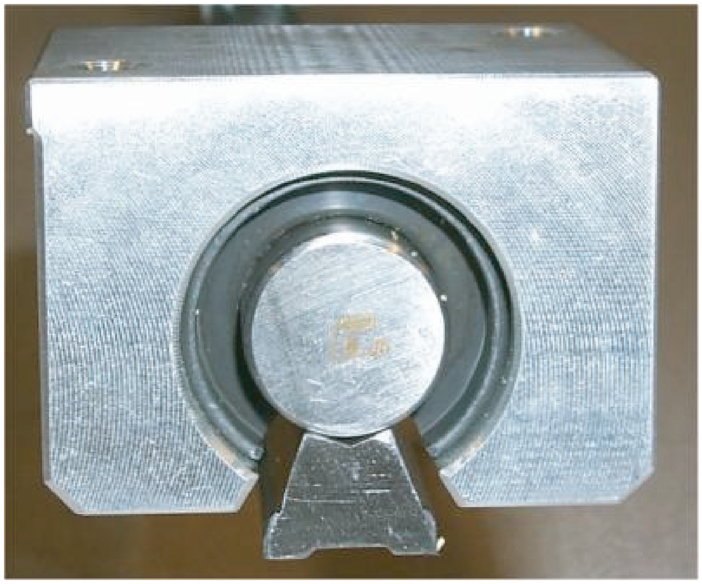

Figure 4.4: End View of Ceramic Bearing and Pillow Block on Shaft

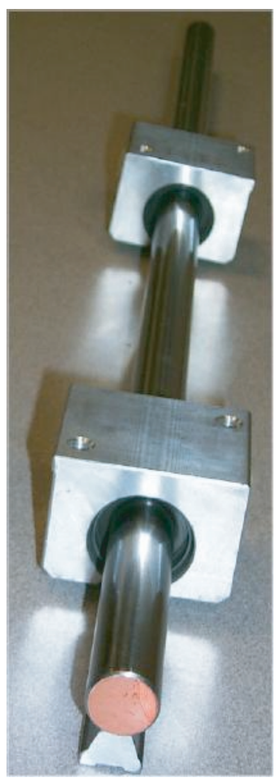

Figure 4.5: Assembly of Bearings on Shaft

the piston needs to come very close to the roof of the cylinder at TDC. If the piston were to impact the head, expensive damage could be done to the valving or the combustion chamber. This means that there is a very short distance between the extreme of motion necessary for regular service and the position where the dynamic assembly must be brought to a dead stop. This distance was approximately 5mm, and stopping the moving assembly from full speed over this distance would require a large shock. Assuming a worst case scenario is the motor applying full force upward and the dynamic assembly traveling at 5.24m/s upward, and that the stop exerts a constant force over the 5mm stroke, the force necessary to stop the dynamic assembly is:

$$F = \frac{\frac{1}{2}mv^2}{\Delta x} = \frac{\frac{1}{2}(16kg)(5.24m/s)^2}{.005m} = 43.9kN \tag{4.1}$$

Which yields a constant deceleration of:

$$\ddot{x} = \frac{F}{m} = \frac{43.9kN}{16kg} = 280G \tag{4.2}$$

This is a large acceleration, but not excessive when compared to some of the other accelerations in the normal duty cycle of the linear engine. Devoting a 100mm by 100mm area to the energy absorbent device, the crush strength required is:

$$\sigma_{crush} = \frac{F}{A} = \frac{43.9kN}{.01m^2} = 4.4MPa \tag{4.3}$$

This is an unattainably large force per unit area for most nondestructive means of slowing a device. Considering destructive means, a material with a crush strength in this range which would exert a relatively constant predictable force as it was crushed would be ideal. The most common such material for energy absorption applications is aluminum honeycomb. With a carefully metered precrush, aluminum honeycomb exhibits a nearly constant crush strength until the cells fully collapse

Figure 4.6: Aluminum Honeycomb Material

upon one another, at which point the material behaves more like solid aluminum. In between the precrush and this full collapse, a sheet of honeycomb starting at a thickness of about 12mm will have a stroke of 5mm. Free samples were obtained from Alcore, with a thickness of 15.9mm (which may be modified by machining) and a rated crush strength of 5.9MPa (see fig. 4.6.) A square area of this material with sides of 86mm would be sufficient to stop the linear engine.

At the other extreme of movement, there was little to limit the distance over which the assembly must be stopped. A distance of 50mm would be more than sufficient to bring the dynamic assembly to a soft stop. Viscous shock absorber technology is well suited to these conditions. For the linear engine application, three failure modes were considered (see table 4.1.) The first mode corresponded to the accidental application of full force to the motor at zero velocity. The second corresponded to a peak velocity typical of normal service accompanied by a moderate force from the motor or piston. The final case considered a power failure at the moment of combustion, where the piston would accelerate downward with a peak velocity of 8.5m/s, but with force due

Case	Force	Velocity
I	9.50 kN	0.0 m/s
II	1.00 kN	5.0 m/s
III	0.15 kN	8.5 m/s

Table 4.1: Failure Modes Necessitating Shock Absorber

Figure 4.7: Shock Absorber

only to the weight of the dynamic assembly.

The velocities necessary for the linear engine application were higher than typical for shock absorbers, so most suppliers we consulted suggested a custom device. This led to a steep increase in price from some vendors, but EfDyn was able to meet the specs for $190, comparing favorably to other quotes. Therefore, a modified version of EfDyn shock model SAS .75x2-BS-04-25 was selected (see fig. 4.7.)

Figure 4.8: Power Cable, Olflex Model 891004CY

4.3 Dynamic Cabling

Two electric cables extend from the rear of the coil. One transmits power to the coil via four conductors, and the other communicates signals from the hall effect sensors and the temperature sensor to the amplifier over five wire pairs. Each conductor on the power cable must be capable of carrying $30A_{rms}$, which corresponds to the maximum continuous rating for the coil. Shielding is important for both cases, in order to minimize EMF emissions and interference.

Aerotech recommended Olflex as a supplier for high flexibility cabling. Their representatives indicated that 10 AWG wire was sufficient for the coil's power needs. For effectively infinite life, a minimum bend radius must be observed. Model 891004CY, which has a minimum bend radius of 188mm, was selected as the power cable (see fig. 4.8.) Model 35902, with a minimum bend radius of 65mm, was chosen to carry the signals (see fig. 4.9.)

Figure 4.9: Signal Cable, Olflex Model 35902

4.4 Mechanical Design

In order the integrate these components, the mechanical design of the system was investigated. The goal of this design was not to fully determine the details necessary to fabricate the linear engine, but rather to suggest how the system could practically be laid out. The most critical task of the mechanical design is to align the two shafts to each other, the magnet ways, and the top plate. Additionally, the dynamic portion must be able to withstand large loads with minimal mass. Designing the static assembly for strength is not as difficult, for there is no incentive to reduce weight other than cost.

Much of the alignment is facilitated by the use of a precision ground plate (see fig. 4.12.) The shafts are bolted to this plate via the shaft supports. Two milled steel bars separate the magnet ways from the plate via the appropriate distance. This subassembly may be put together, aligned, and tested separate from the rest of the system.

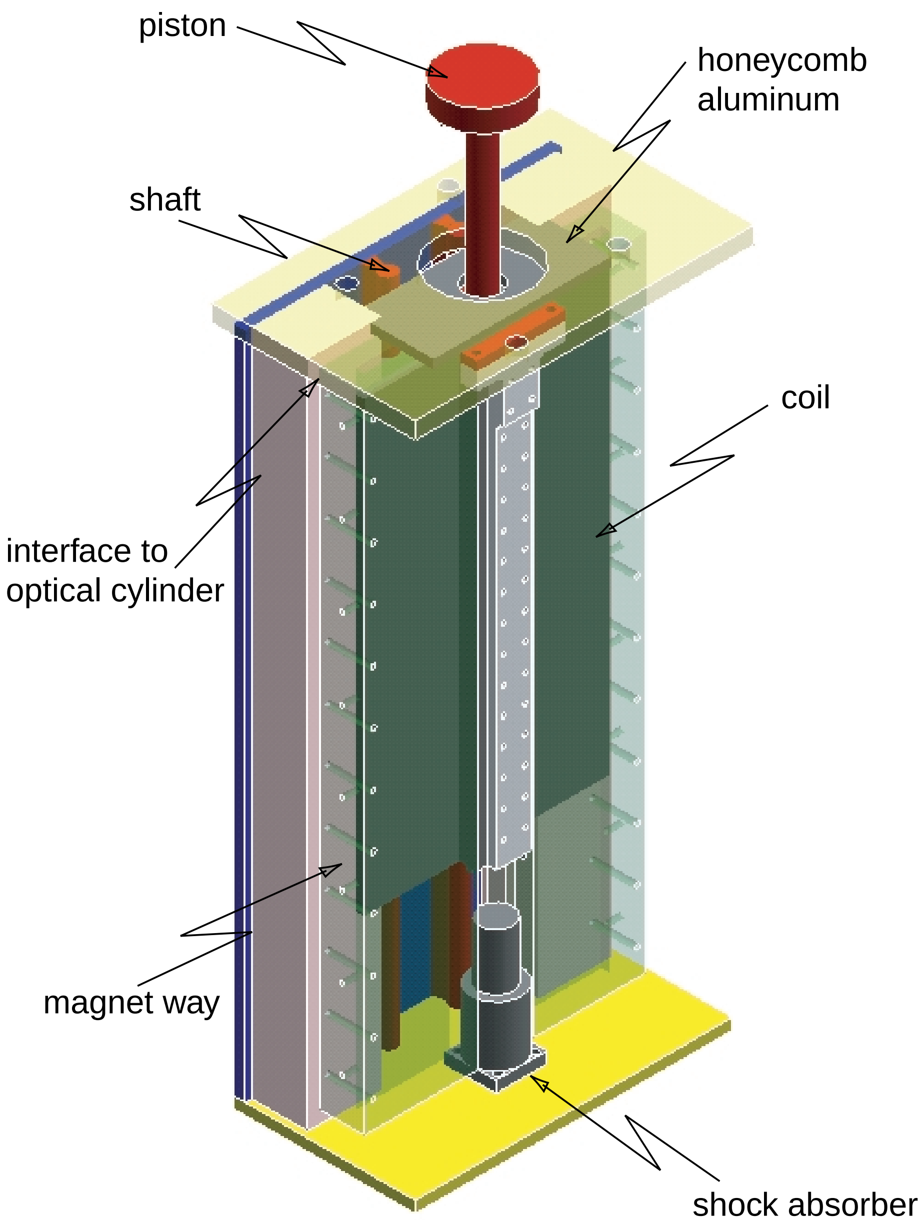

Figure 4.10: Isometric View of Full Assembly

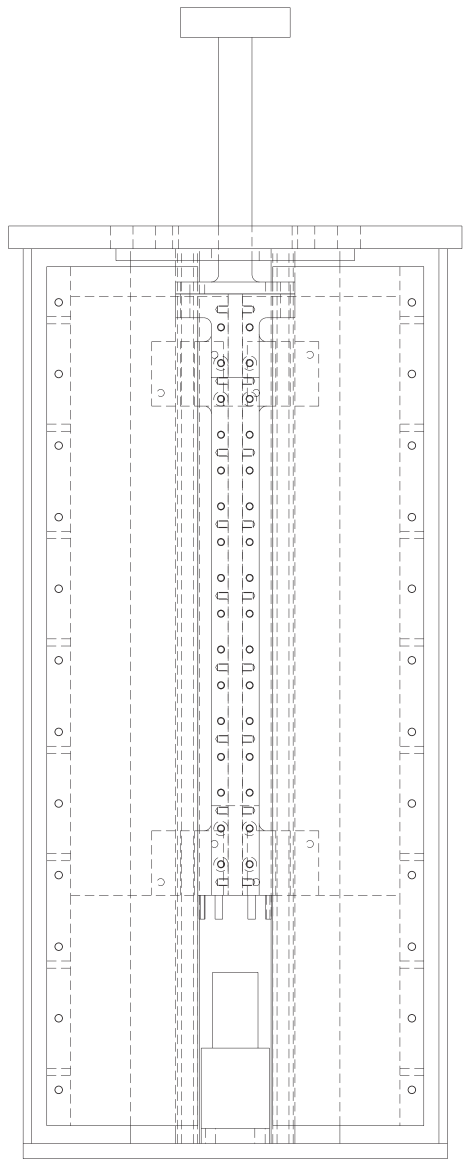

Figure 4.11: Hidden Line View of Front of Full Assembly

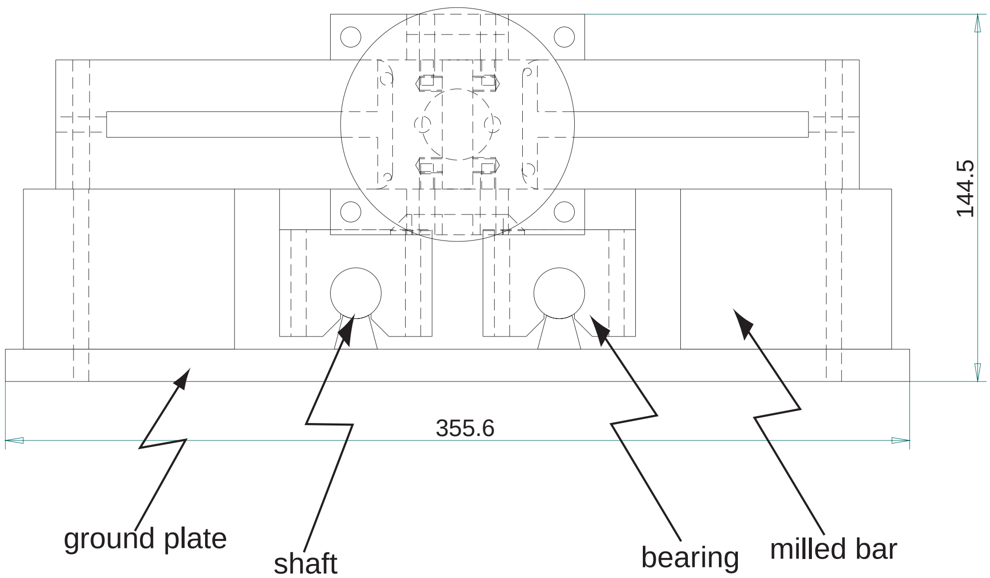

Figure 4.12: Top View Showing Components Requiring Precision Alignment

The dynamic portion presents some other issues. One is the area required to withstand the peak forces. Considering the worse case scenario of a 7 MPa peak pressure in the cylinder, the force on the piston would be:

$$F_{piston} = pA = (7 \cdot 10^6 Pa)(.0066m^2) = 46.2kN \tag{4.4}$$

If the piston is made of 7075-T6 aluminum, with a fatigue limit of 158MPa, then the minimum area would be:

$$A_{min} = \frac{46.2kN}{158MPa} = 297mm^2 \tag{4.5}$$

Therefore, a diameter of 30mm would yield a safety factor of 2.4:

$$SF = \frac{A}{A_{min}} = \frac{297mm^2}{\left(\frac{30mm}{2}\right)^2 \pi} = 2.4 \tag{4.6}$$

This is the diameter chosen for the rod portion of the piston. The rest of the

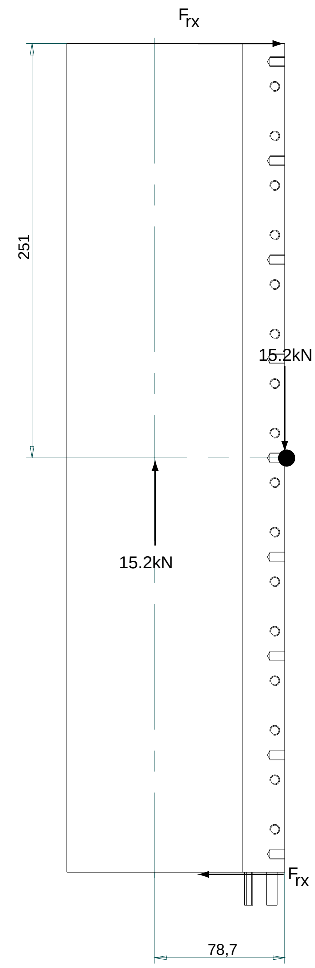

Figure 4.13: Free Body Diagram of Coil

assembly joining the coils has a cross sectional area of at least $800mm^2$ (compared to $707mm^2$ for the 30mm rod,) so it should also suffice.

Another difficult issue is fastening the coils to the rest of the dynamic assembly. In order to understand this problem, it was necessary to make a free body diagram for the coil (see fig. 4.13.) Applying equation 3.22 to the above worst case scenario, with the motors at maximum force, the acceleration is:

$$\ddot{x} = m^{-1}(F_{piston} - F_{mot}) = \frac{46.2kN - 9.5kN}{16kg} = 2300m/s^2 \tag{4.7}$$

Each coil has a mass of 4.45kg, so the total force which each is opposing is:

$$F = m\ddot{x} + F_{mot} = (4.45kg)(2300m/s^2) + 4.7kN = 15.0kN \tag{4.8}$$

This is the shear force which the fastening arrangement must withstand. This is somewhat problematic, because very few modifications may be made to the coil without damaging it, and the existing interface consists of 10mm deep M6 holes tapped in aluminum. The threaded fasteners which would use these holes are not effective at resisting shear forces. A partial solution may be to support this load on the face at the end of the coil, since the loads will be much smaller in the opposite direction.

Additionally, there are significant forces trying to separate the two coils at the bottom of the assembly. These can be found by summing the moment on each coil, around the center indicated by the solid black circle. Because the center piece is balanced, the downward force may be considered to act at the edge of the coil:

$$\sum M = (15.2kN)(78.7mm) - (2)(251mm)F_{rx} = 0 \tag{4.9}$$

Yielding $F_{rx} = 2.4kN$, if the entire load could be applied to the extreme of the coil length. This load is less problematic than the shear forces, since it may be applied axially to threaded fasteners. If failure occurs in the tapped aluminum, and one assumes that a single thread must bear the full load, then the equation [17]

$$A_s = \pi d w_0 p \tag{4.10}$$

applies, where A_s is the shear area, d is the diameter, w_0 is an "area factor", and p is the pitch. For M6 holes, this yields:

$$A_s = \pi(6.0mm)(0.88)(1.0mm) = 1.710^{-5}m^2 \tag{4.11}$$

For 6061 T6 aluminum, the yield stress in shear is 159MPa [17], yielding:

$$F = S_{ys} A_s = (159Mpa)(1.710^{-5}m^2) = 2.7kN \tag{4.12}$$

This is above the maximum force calculated above, but does not leave much of a safety factor. The final design must take care in the detail design of the fasteners for axial loading.

Chapter 5

Closure

The essentials of the design of a linear engine have been presented. In this final chapter, the linear motor, the electrical subsystem, and the mechanical subsystem are once more addressed in order to discuss the quality of the solution so far and appropriate directions for future work. This discussion is followed by some concluding remarks.

5.1 Linear Motor

The selected linear motor system shows great promise as the electrical machine in the linear engine. The BLMX-502b is lightweight and capable of exerting large forces. Although it is predicted that experimental motion profiles will have to be adapted to accommodate the system's limitations, simulation results suggest that these adaptations are not detrimental to the combustion process and are perfectly acceptable.

Two issues remain open in implementing the linear motor system: how to exert precise control of force despite the variability of k_m, and the thermal characteristics of the coils. The first of these is an issue because it was initially hoped that the voltage sent to the BAS-100 amplifier would correspond to a proportional force exerted by the coil, without feedback or compensation. The experimental results discussed in section 3.4 indicate that these relationships are not as simple and predictable as was hoped, especially at small loads.

This problem can be addressed with a pair of related strategies. The first is to perform a more thorough identification of the linear motor system. This would require a new or modified prototyping apparatus, or special allowances to perform identification in the final design. A more flexible means of applying and measuring forces may be necessary, along with a means of automatic data acquisition. This data would be analyzed in order to determine how input voltage to the amplifier is related to force applied by the coil, in the face of varying loads and dynamic conditions. If this model were adequately defined, it is possible that an open loop control scheme could still be implemented.

Another strategy is to provide a means of measuring force during operation and closing the loop. A load cell could be applied in series with the piston, providing a well calibrated sensor right out of the box. This, however, might complicate the mechanical design, and would add some compliance to the system. A less obtrusive means of sensing force would be to apply strain gages to the piston rod, and calibrate these strains to the load. Because the rod is designed for high strength and low compliance, the resulting strains would be very small, complicating measurement. This closed loop strategy would work best if combined with at least some system identification, allowing sensor accuracy to be augmented by a thoughtful observer design.

The second open issue is determining the thermal characteristics of the coils. These are of great importance, for they determine the maximum RMS current which may be safely passed through the coil, as well as the duration over which the peak current may be sustained. Aerotech specifies a value for thermal resistance, but in practice, this will vary according to the components attached to the coils. No specification is made for the thermal capacity, which determines how quickly the coils will heat up for a given power input. In order to guarantee safe operation at the limits of performance, it will be necessary to experimentally test these thermal parameters. In order to accomplish this, a known current must be applied across the stationary coils, which could be accomplished using the BAS-100 amplifier. Additionally, there must be a means for measuring the temperature of the coils. There are two salient solutions to this problem: one or more temperature sensors, such as thermocouples, may be applied to the surface of the coils, or the resistance of the coils themselves, which should be proportional to temperature, could be measured.

5.2 Mechanical Subsystem

The selected bearings promise to be an effective solution. They have good wear characteristics, reasonable friction levels, excellent tolerances, and require little maintenance. Because they have a single moving part, shock should not be an issue (tolerances help too.) They remain to be proven, perhaps with some testing plan.

Effective energy absorbtion solutions have been identified for the top and the bottom of the linear engine's stroke. At the top, the design dictates that the piston must stop over a very short distance, and this cannot be easily avoided without imposing severe limits on the compression ratio. Given this short distance, the honeycomb aluminum is an excellent solution. At the bottom of the stroke, a longer distance is available over which to decelerate the dynamic assembly. The selected shock absorber has the capacity to bring this assembly to a gentle stop in each of the likely failure modes.

The overall mechanical design remains in an early formative stage. A means of fastening the coils to the dynamic assembly will require special attention. Some modifications to the coils are possible; Aerotech specifies that the holes on top, except the two pairs nearest where the cable exits the coil and the single pair at the opposite extreme, may be drilled out to an 8mm diameter. However, they recommended against other modifications, especially to the holes on the sides, limiting the design space for fastener solutions. Additionally, a structure to anchor the linear engine to the floor will need to be designed. This problem suggests some kind of welded frame, but care must be taken to assure this frame has the necessary tolerances to interface accurately with the rest of the linear engine.

In the future, if it is desired to move in the direction of a practical power source, the opposed piston design has some advantages. Linear motors, as with other electrical machines, operate inefficiently near stall conditions. If the linear motor is to be used to fully reverse the velocity of the piston, it must add significant mechanical energy to the system near stall, resulting in large resistive losses. In an opposed piston design, the velocity is always reversed by a combustion event. Unfortunately, this design cannot be applied without limiting the possible motion profiles of the piston, and necessitates a 2 stroke working cycle. A spring at the bottom of the stroke, especially one with a variable rate, could also improve system performance around stall conditions. The key disadvantage to this strategy, relative to the opposed piston design, is that it adds mechanical complexity without increasing the thermodynamic capacity of the engine.

5.3 Electrical Subsystem

The Renishaw RGH41T meets all the specifications necessary for the linear engine, and has already been proven to some extent in the linear motor prototype. A less expensive encoder with lower resolution but the same velocity capability might be desirable, if one exists.

The Olflex high flexibility cabling has enough current capacity for the power needs of the application, and enough conductors to carry the necessary signals. The cables have not yet been tested. In the final mechanical design, allowances will have to be made to assure that the minimum bend radii are observed. One common design to guarantee that the bend radii are maintained is illustrated in fig 5.1.

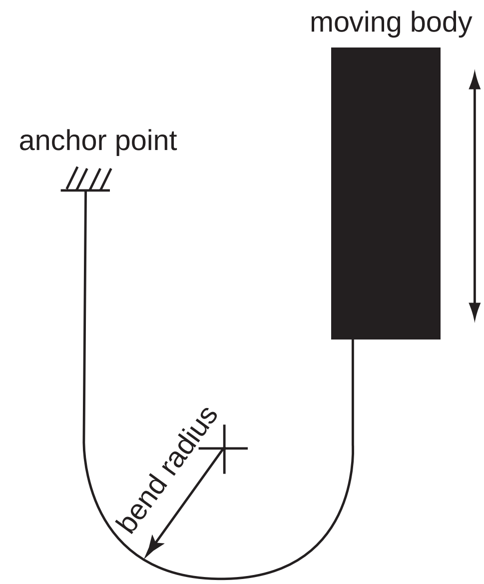

Figure 5.1: High Flexibility Cable

A first attempt at a control system has been developed in simulation. This controller will require an electronic system for implementation. Because data logging and decision making functions will need to be integrated with the control system, implementing the controller in discrete form on a computer is the most practical strategy. Single board PC's from Versalogic have been proven effective for tasks requiring bandwidth of several kHz in experiments on the VVA apparatus, and this established platform should also be adequate to the computing needs of the linear engine.

The final controller design will follow from the needs of experiments. It may be that a position controller similar to the one used in simulation will be ideal, or a controller which tracks such parameters as pressure, temperature, or mass flow may be desirable. The dynamics involved in closing the loop around these quantities are more complicated than those of the existing controller, and more advanced techniques from nonlinear controls may be necessary.

Another problem in implementing the control system is actuator saturation. While the only way to completely eliminate this issue is to increase the actuator capacity (i.e., purchase $9,000 to $17,000 more of linear motors), there are a few techniques which can be applied to improve controller performance despite saturation.

One problem related to saturation is integrator windup [19, 23]. In order to assure accurate tracking on a linear controller designed to correct for small disturbances, the gain on the integrator term may be large. When the actuator saturates, significant errors may be sustained until the desired output is once again within the actuator's capability, leading to very large integrator values. One proposed solution to this problem is to use an "error governor" or "measurement governor". These strategies scale the input to keep the output just below the point of saturation.

Another strategy for dealing with saturation is presented independently by Pappas [18] and Warnick [22]. They describe systems in which a desired trajectory is known for all time. This trajectory is then remapped variably to time, via an additional parameter. The new mapping is designed such that the control output never saturates, and the desired trajectory is synchronized to the additional parameter. Because the piston position in the linear engine may be synchonized to an equivalent crank angle, which may have a variable relation to time, this strategy makes a lot of sense.

5.4 Conclusion

While it is likely that this engine will not be capable of net generation of power, it is a good platform to study phenomena which may lead to improved linear engines for power generation. This apparatus would be unique in providing the ability to conduct experiments with varying piston motion profiles, independent of any crankshaft or coupled second piston, at a scale comparable to traditional research engines.

Clearly, much remains to be done in order to implement the linear engine apparatus. After the last technological hurdles are overtaken, significant additional investment in design, fabrication, testing, and experimentation will be necessary before the apparatus can yield any practical results, and it might be the case that additional iterations on the the device will be needed. It will not be possible to fully test the efficacy of the linear engine until it is completely realized, but the feasibility of continuing along this path has been established.

Appendix A

Prototype Dimensional Drawings

1. Bottom Plate
2. Bracket Side Pieces
3. Breakout Box
4. Encoder Support
5. Yoke
6. Bracket Joiner
7. Aluminum Plate
8. Side Plates
9. Motion Stops
10. Cable Stress Relief
11. Top Plate

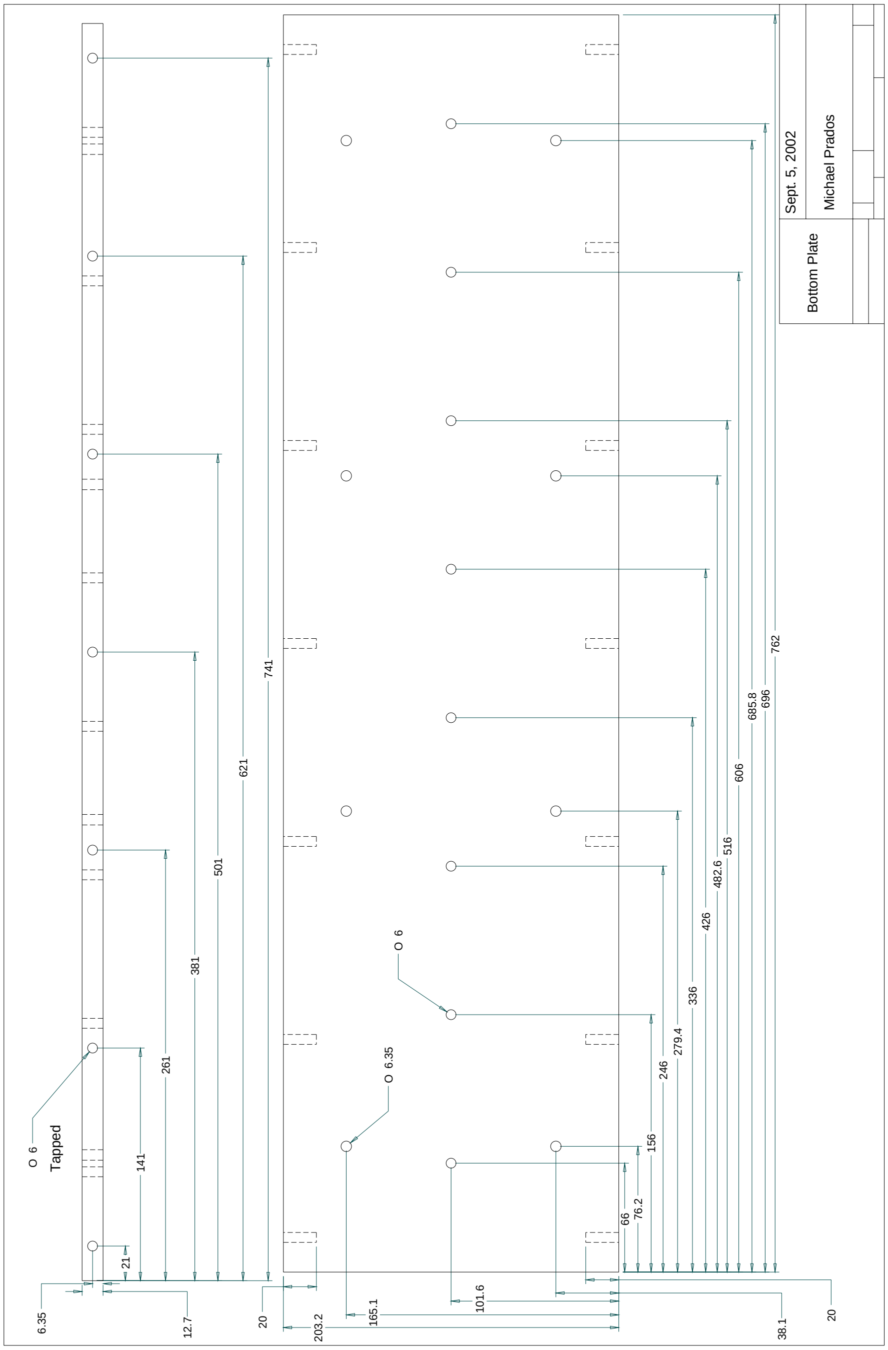

Figure A.1: Bottom Plate

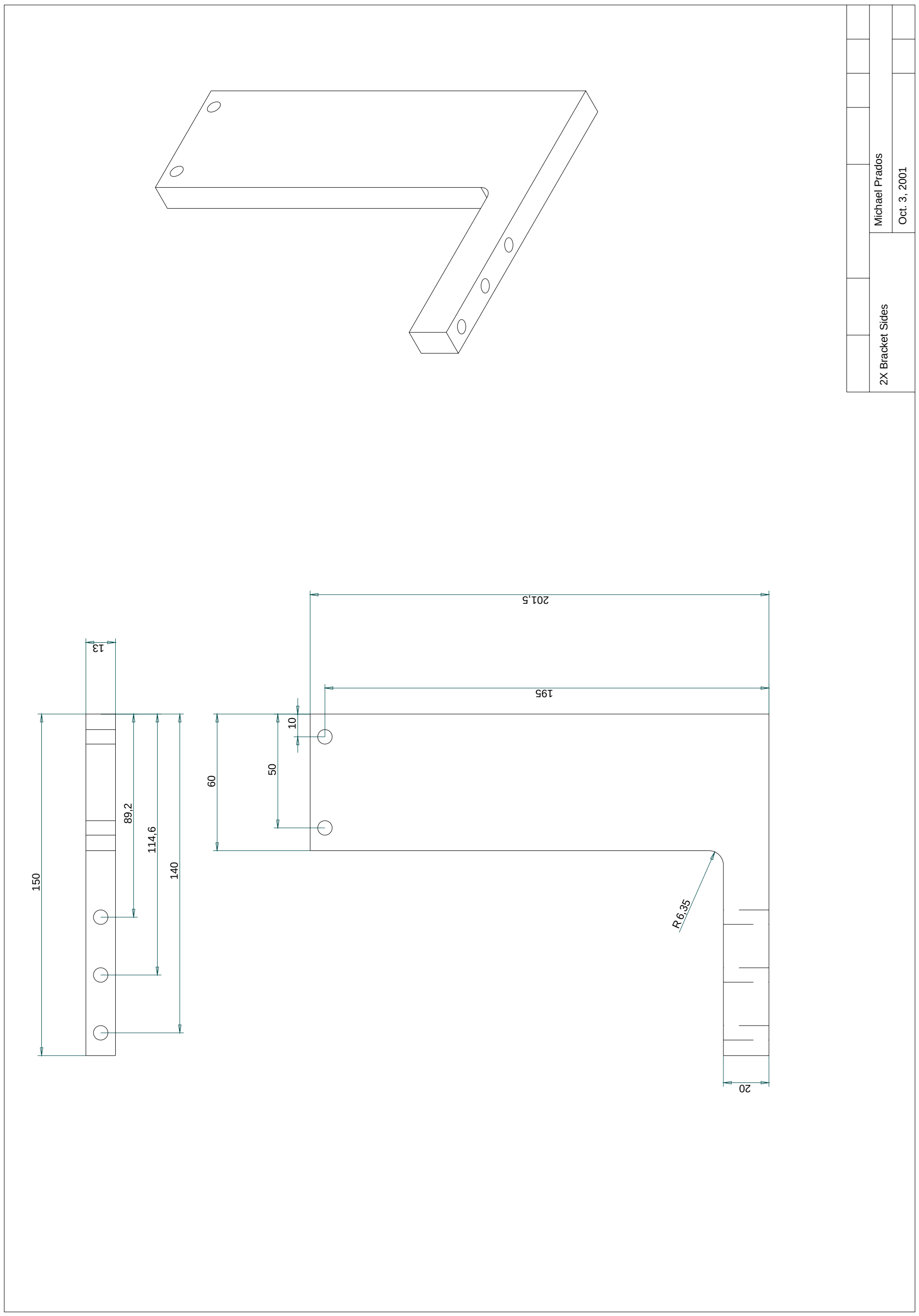

Figure A.2: Bracket Side Pieces

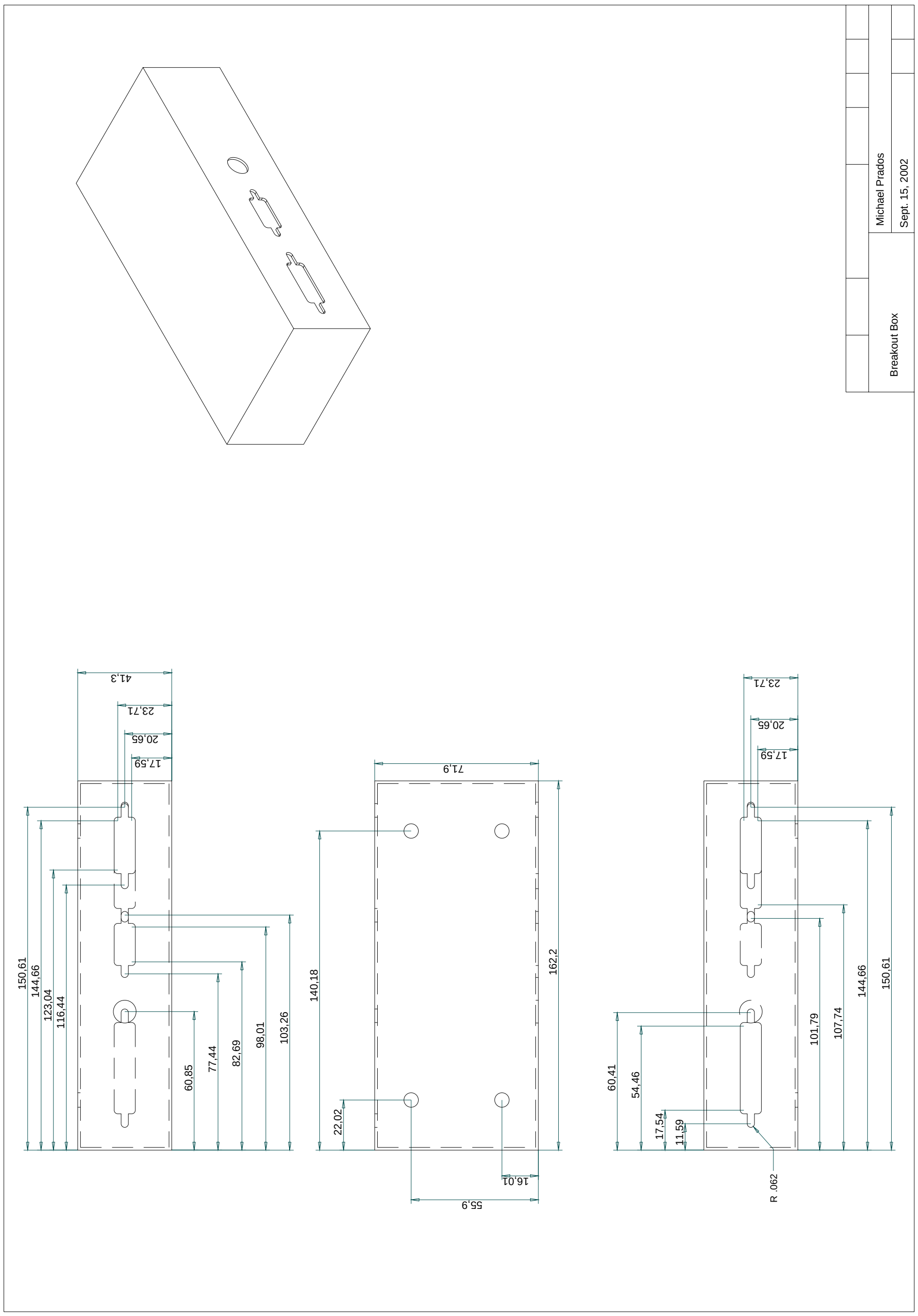

Figure A.3: Breakout Box

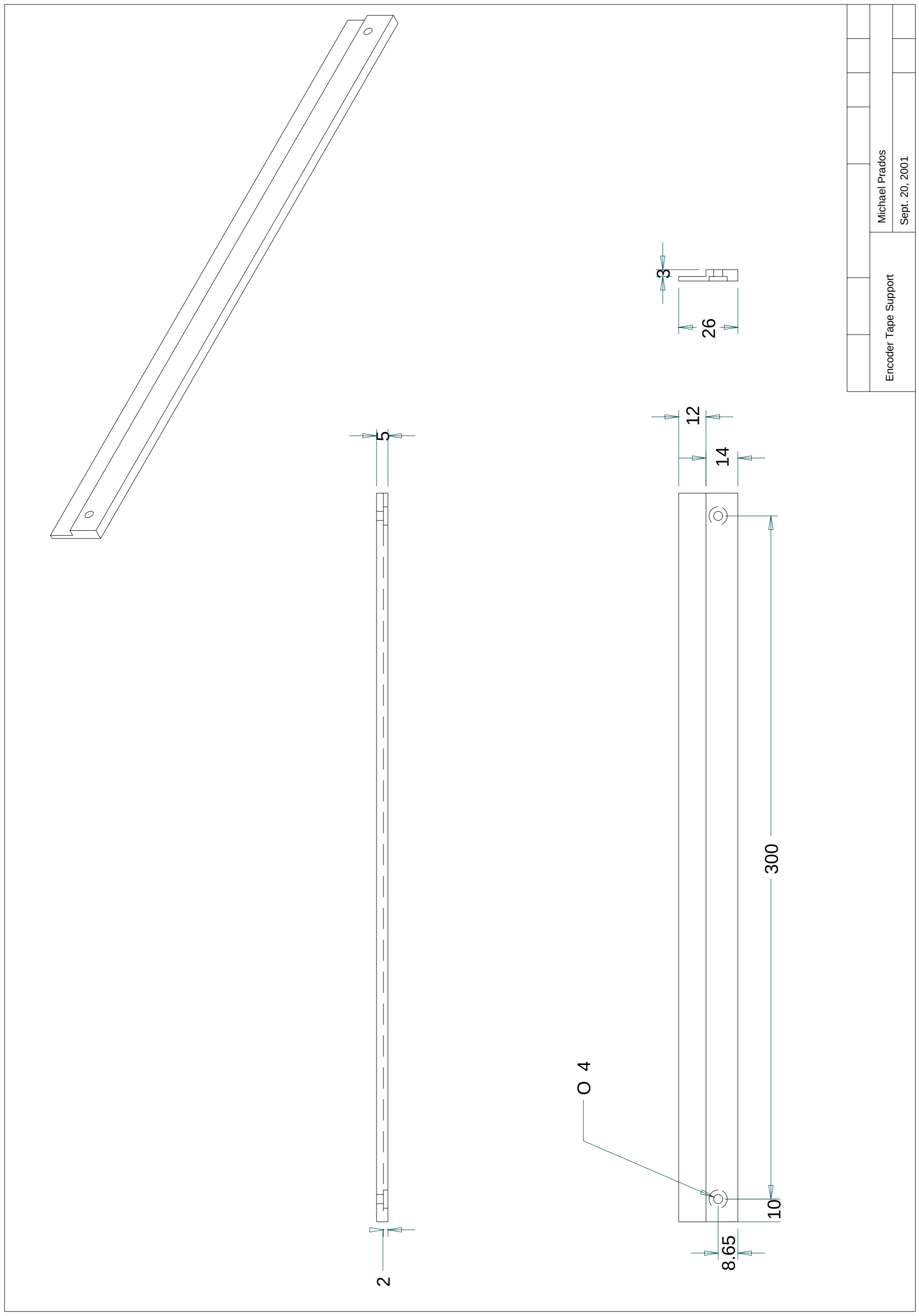

Figure A.4: Encoder Support

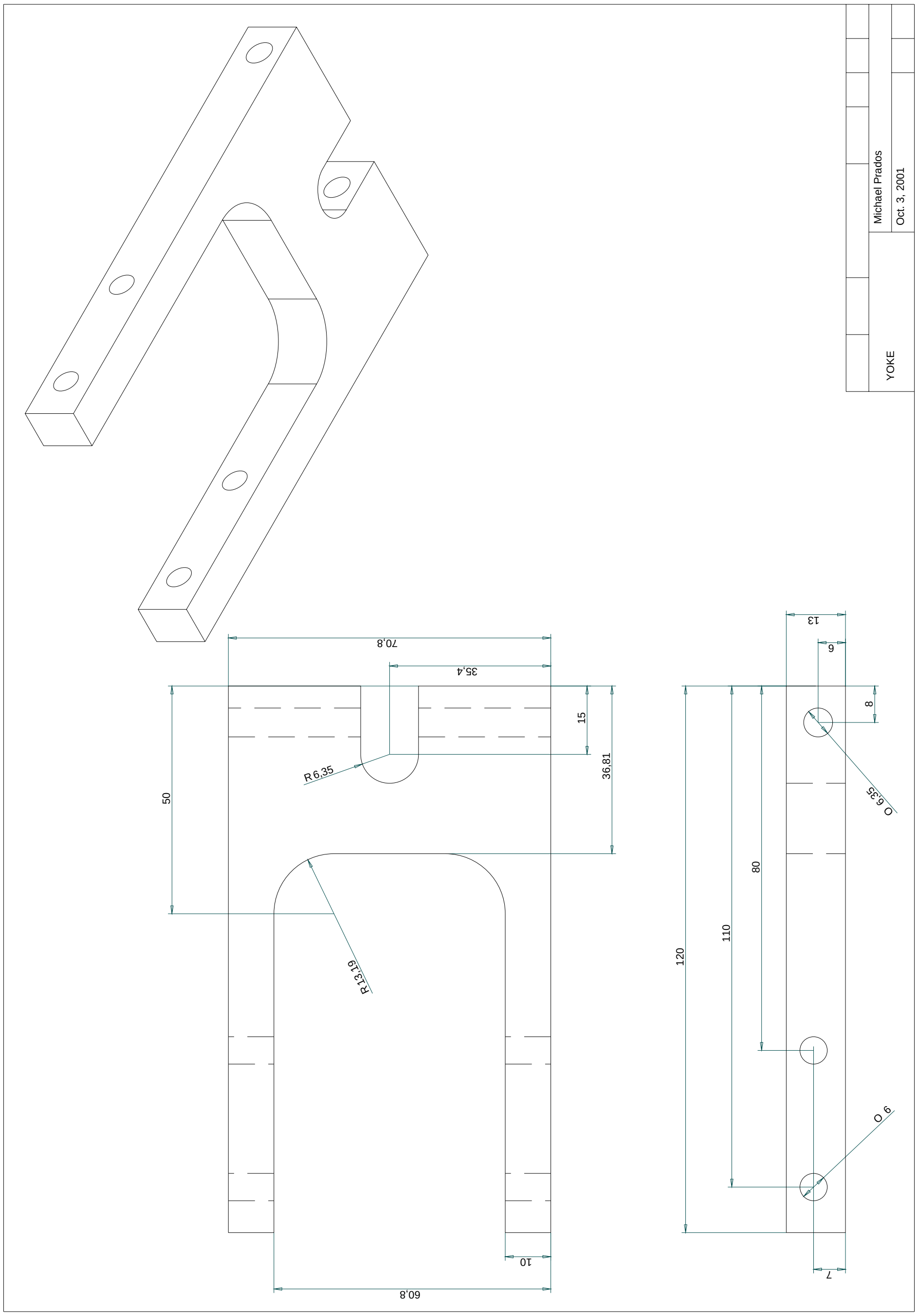

Figure A.5: Yoke

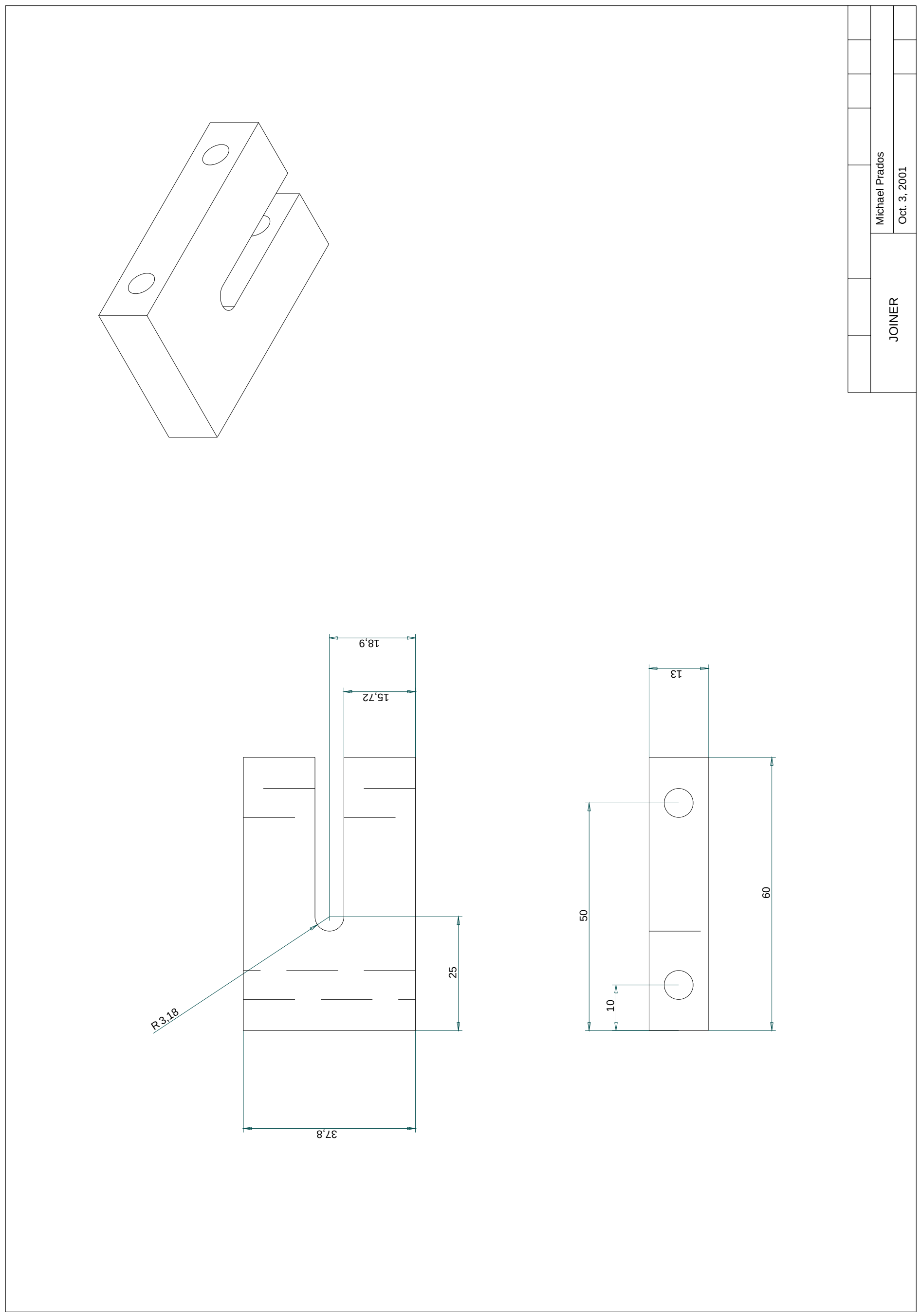

Figure A.6: Bracket Joiner

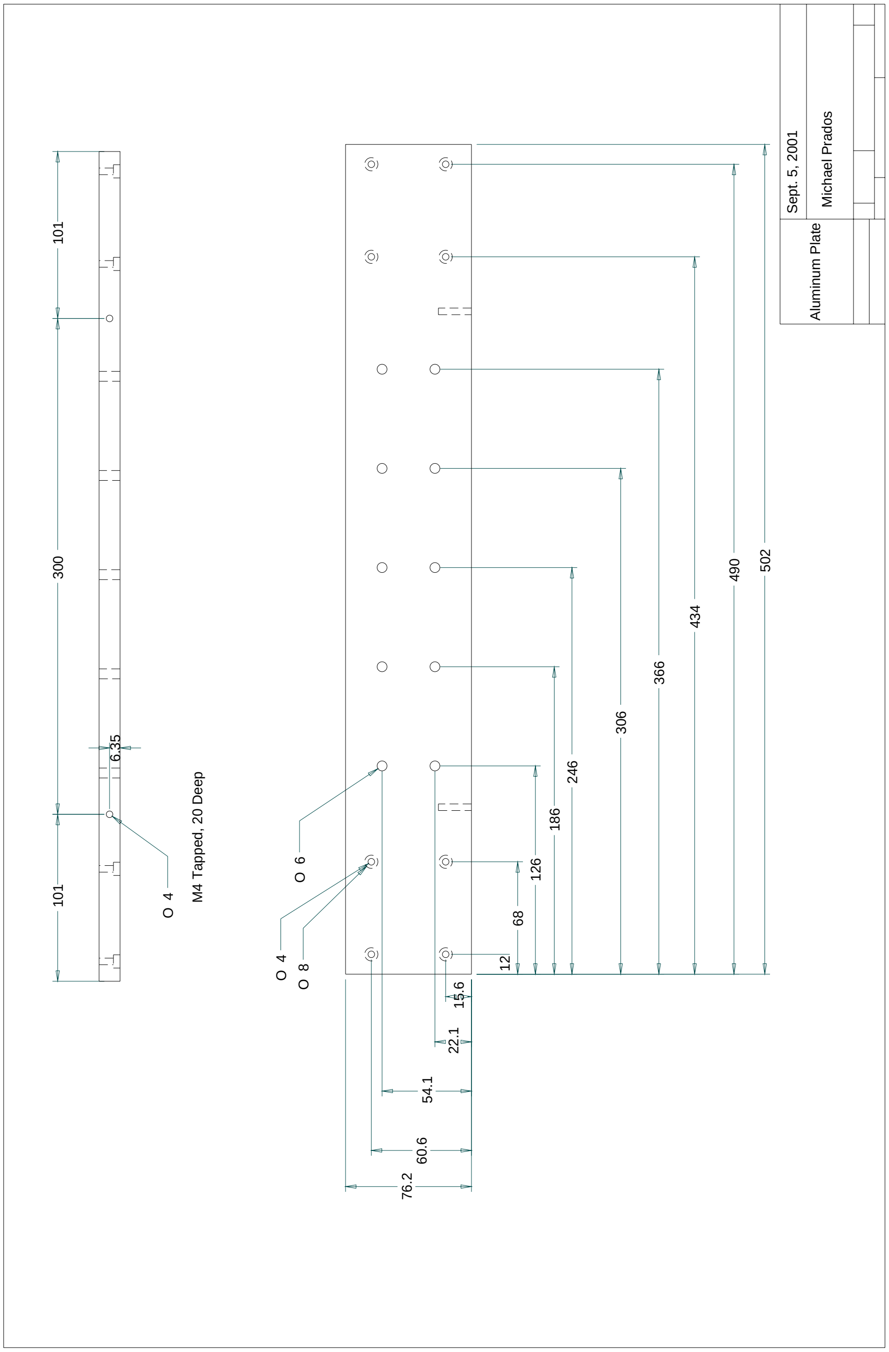

Figure A.7: Aluminum Plate

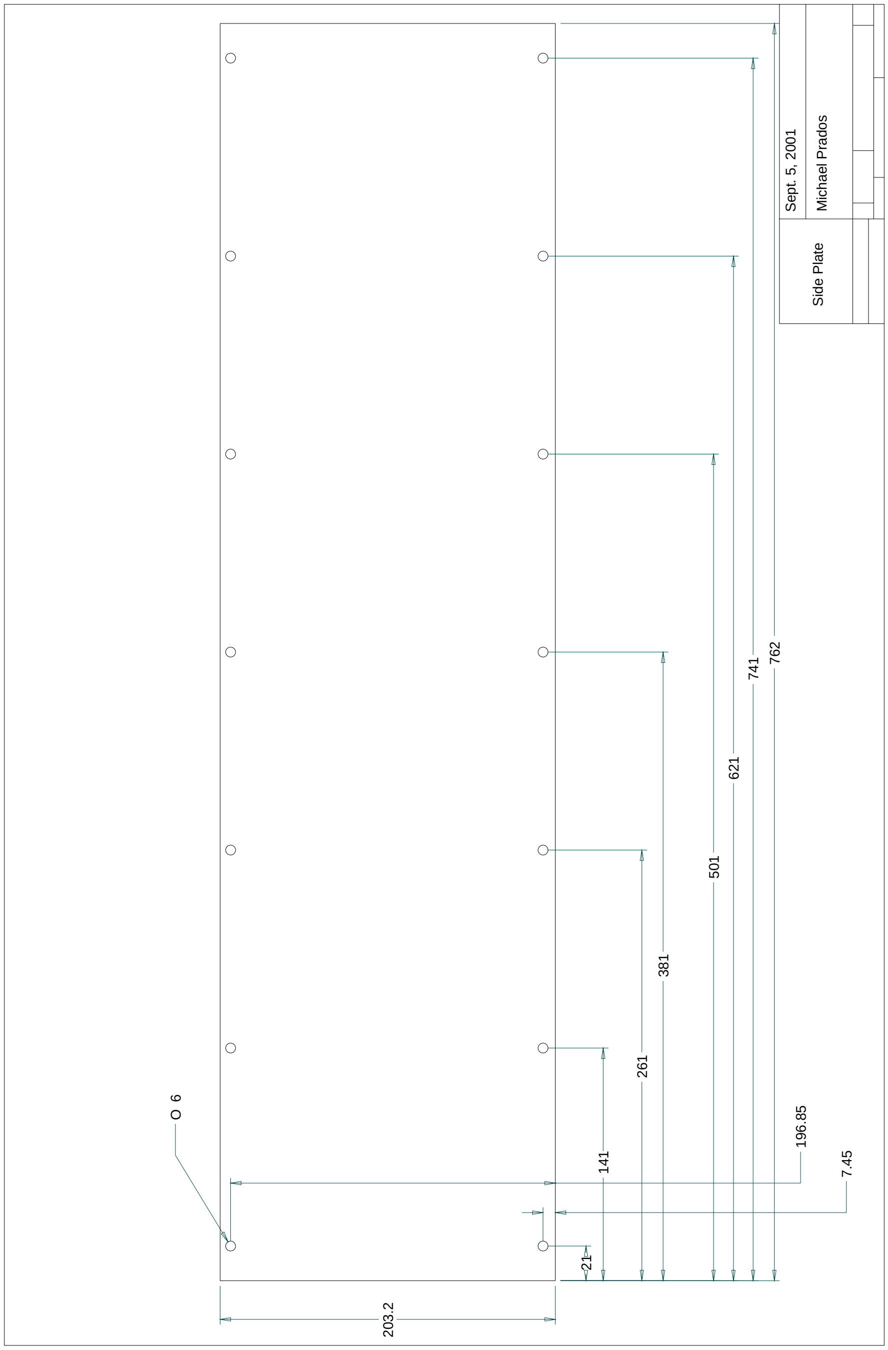

Figure A.8: Side Plates

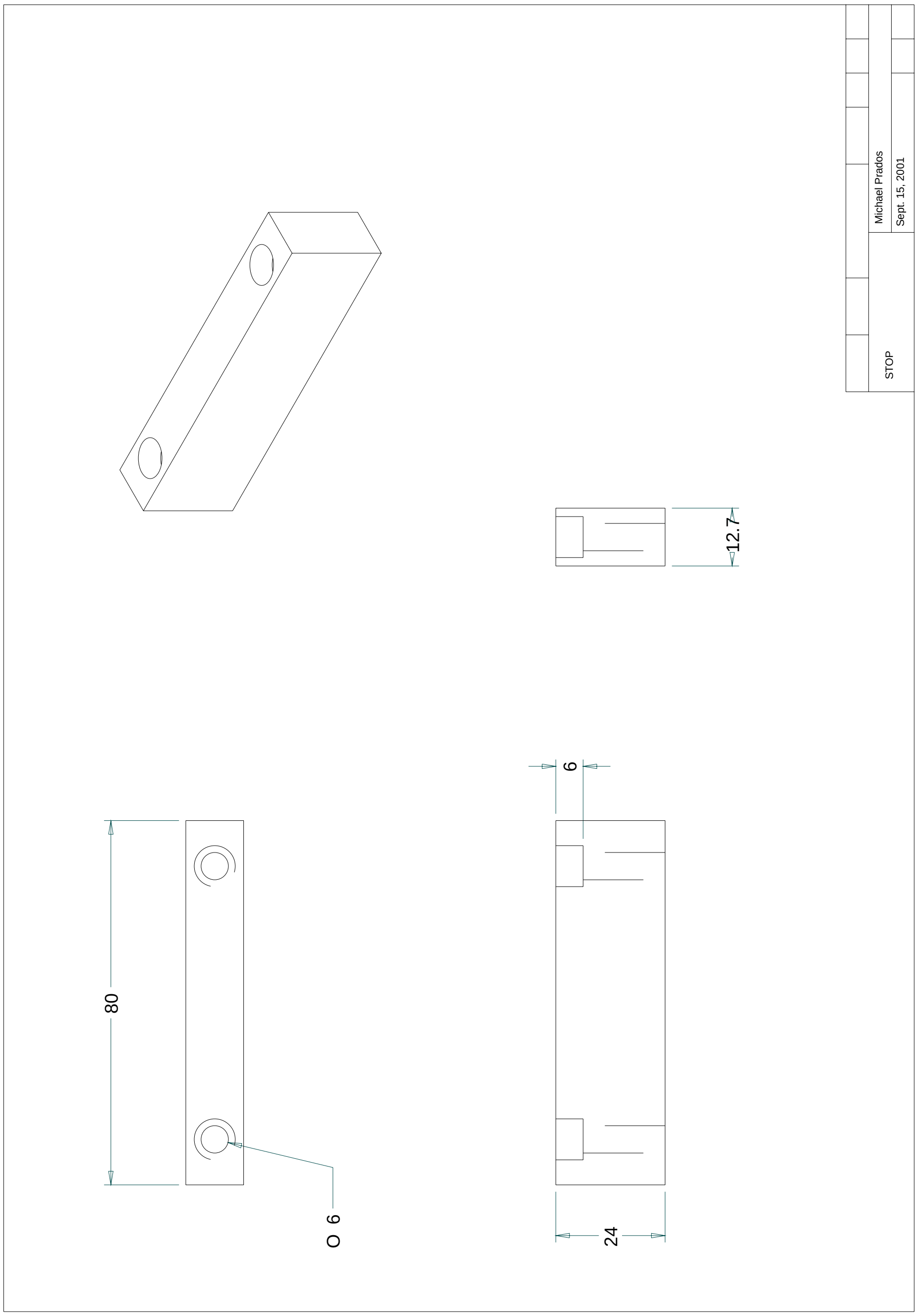

Figure A.9: Motion Stops

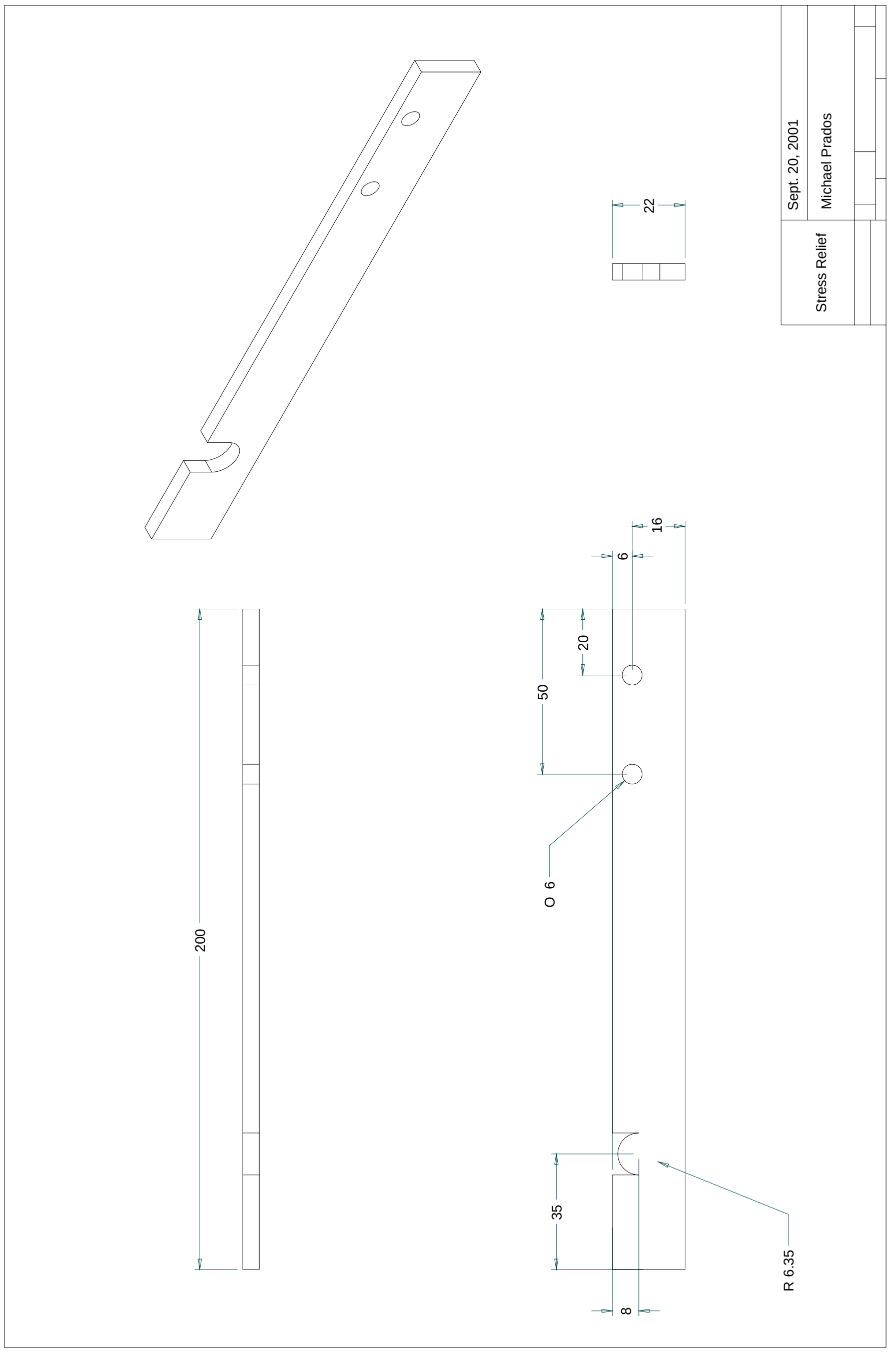

Figure A.10: Cable Stress Relief

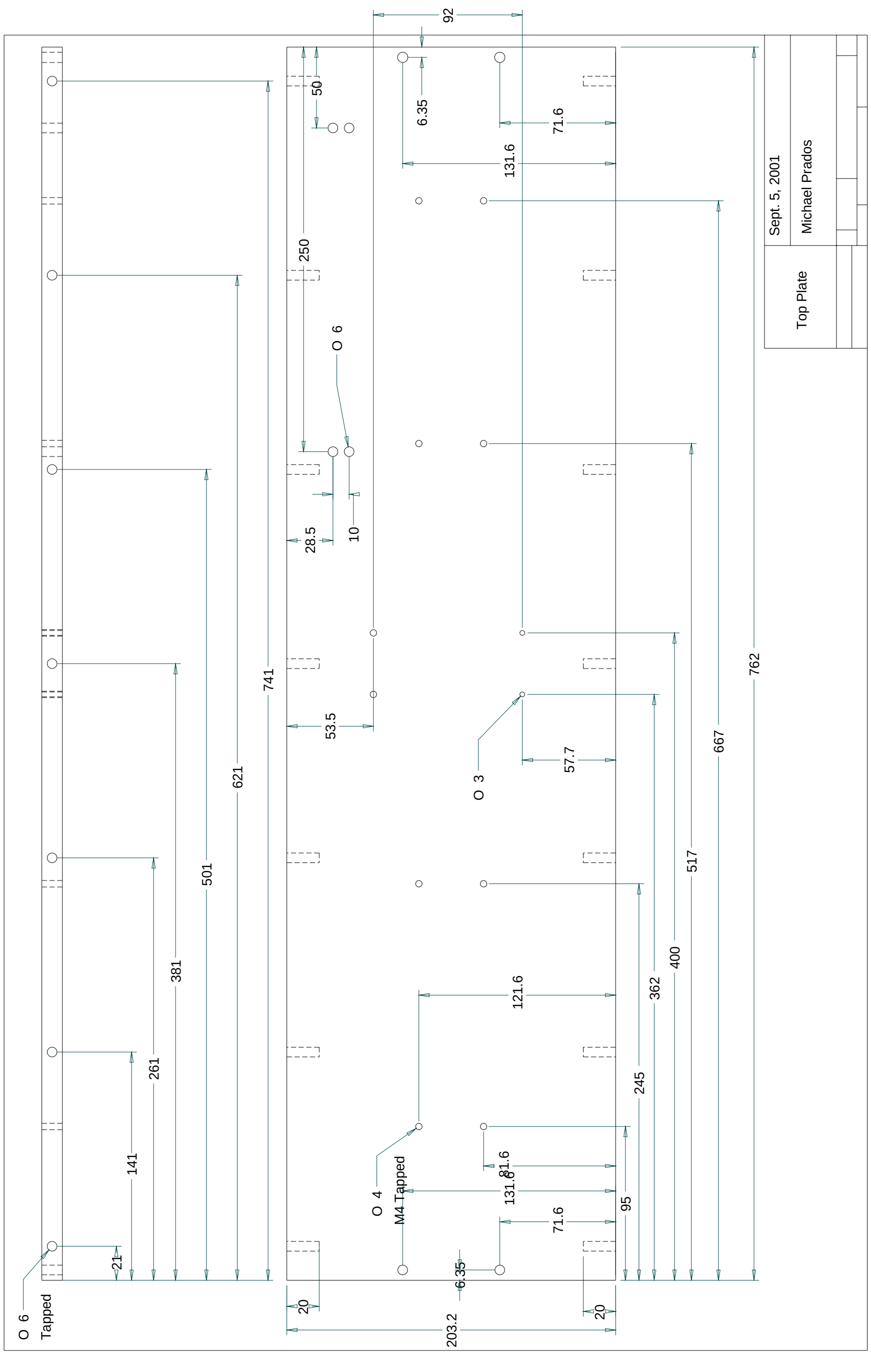

Figure A.11: Top Plate

Bibliography

[1] Peter A. J. Achten. A review of free piston engine concepts. Technical Report 941776, SAE Technical Papers Series, 1994.

[2] Christopher M. Atkinson, Sorin Petreanu, et al. Numerical simulation of a two-stroke linear engine-alternator combination. Technical Report 1999-01-0921, SAE Technical Paper Series, 1999.

[3] I. Boldea and S. A. Nasar. Permanent magnet linear alternators part I: Fundamental equations. *IEEE Transactions on Aerospace and Electronic Systems*, AES-23(1), 1987.

[4] I. Boldea and S. A. Nasar. Permanent magnet linear alternators part II: Design guidelines. *IEEE Transactions on Aerospace and Electronic Systems*, AES-23(1), 1987.

[5] Nigel N. Clark, Parviz Famouri, et al. Modeling and development of a linear engine. In *1998 Spring Technical Conference of the ASME Internal Combustion Engine Division*, volume 30-2, April 26-29, 1998.

[6] Jonathan Adam Dawson. *An Experimental and Computational Study of Internal Combustion Engine Modeling for Controls Oriented Research.* PhD thesis, The Ohio State University, 1998.

[7] Parviz Famouri, William Clark, Nigel Clark, et al. Design and testing of a novel linear alternator and engine system for remote electrical power generation. In *IEEE Engineering Society, Winter Meeting*, volume 1, 1998.

[8] David E. Foster. An overview of zero-dimensional thermodynamic models for ic engine data analysis. Technical Report 852070, SAE Technical Paper Series, 1985.

[9] D. N. Frey, P. Klotsch, and A. Egli. The automotive free-piston-turbine engine. *SAE Transactions*, 65:629–634, 1957.

[10] Ari Glezer and Mark G. Allen. Miniature reciprocating combustion-driven machinery. United States Patent 6109222, August 29 2000.

[11] Scott Goldsborough and Peter Van Blarigan. A numerical study of a free piston IC engine operating on homogenous charge compression ignition combustion. Technical Report 1999-01-0619, SAE Technical Papers Series, 1999.

[12] William H. Hayt, Jr. *Engineering Electromagnetics*. McGraw-Hill, Inc., 1989.

[13] John B. Heywood. *Internal Combustion Engine Fundamentals*. McGraw-Hill, Inc., 1988.

[14] N. B. Kaahaaina, A. J. Simon, P. A. Caton, and C.F. Edwards. Use of dynamic valving to achieve residual-affected combustion. Technical Report 2001-01-0549, SAE Technical Paper Series, 2001.

[15] Joseph F. Kos. Computer optimized hybrid engine. United States Patent 5002020, March 26 1991.

[16] Denny K. Miu. *Mechatronics: Electromechanics and Contromechanics*. Springer-Verlag, 1992.

[17] Robert L. Norton. *Machine Design, An Integrated Approach.* Prentice-Hall, 1996.

[18] George J. Pappas. Avoiding saturation by trajectory reparameterization. In *Proceedings of the 35th IEEE Conference on Decision and Control*, volume 1, 1996.

[19] Jeff S. Shamma. Anti-windup via constrained regulation with observers. In *Proceedings of the American Control Conference*, volume 4, 1999.

[20] Richard Stone. *Introduction to Internal Combustion Engines.* Society of Automotive Engineers, Inc., 1999.

[21] Peter Van Blarigan, Nicholas Paradiso, and Scott Goldsborough. Homogenous charge compression ignition with a free piston: A new approach to ideal otto cycle performance. Technical Report 982484, SAE Technical Paper Series, 1998.

[22] Sean C. Warnick and Munther A. Dahleh. Feedback synchronization: A relaxation of tracking. In *Proceedings of the American Control Conference*, volume 1, 2000.

[23] Sean C. Warnick and Armando A. Rodriguez. A systematic antiwindup strategy and the longitudinal control of a platoon of vehicles with control saturations. *IEEE Transactions on Vehicular Technology*, 49(3), May 2000.

[24] Xiangqun Zhang. Modeling and simulation of a hybrid engine. Master's thesis, University of Regina, 1997.